APPLICATION OF STIMULI-RESPONSIVE CYSTEINE-BASED ORGANOGELS AS A DRUG DELIVERY SYSTEM FOR CHEMOTHERAPY DRUGS

A THESIS SUBMITTED TO
THE GRADUATE SCHOOL OF NATURAL AND APPLIED SCIENCES
OF
MIDDLE EAST TECHNICAL UNIVERSITY

BY

DIBA ZARE

IN PARTIAL FULFILLMENT OF THE REQUIREMENTS
FOR
THE DEGREE OF MASTER OF SCIENCE
IN
BIOTECHNOLOGY

AUGUST 2023

Approval of the thesis:

APPLICATION OF STIMULI-RESPONSIVE CYSTEINE-BASED ORGANOGELS AS A DRUG DELIVERY SYSTEM FOR CHEMOTHERAPY DRUGS

submitted by **DIBA ZARE** in partial fulfillment of the requirements for the degree of **Master of Science** i**n Biotechnology, Middle East Technical University** by,

Prof. Dr. Halil Kalıpçılar
Dean, Graduate School of **Natural and Applied Sciences** _____

Prof. Dr. Yeşim Soyer Küçükşenel
Head of the Department, **Biotechnology** _____

Assoc. Prof. Dr. Salih Özçubukçu
Supervisor, **Biotechnology, METU** _____

Assoc. Prof. Dr. Emrullah Görkem Günbaş
Co-Supervisor, **Chemistry, METU** _____

Examining Committee Members:

Assoc. Prof. Dr. Batur Ercan
Metallurgical and Materials Engineering, METU _____

Assoc. Prof. Dr. Salih Özçubukçu
Chemistry, METU _____

Assoc. Prof. Dr. Emrullah Görkem Günbaş
Chemistry, METU _____

Assist. Prof. Dr. Melek Parlak Khalily
Basic Science and Health, Yozgat Bozok University _____

Assist. Prof. Dr. Seher Üstün Yaylacı
Medical Sciences, Lokman Hekim University _____

Date: 24.08.2023

I hereby declare that all information in this document has been obtained and presented by academic rules and ethical conduct. I also declare that, as required by these rules and conduct, I have fully cited and referenced all material and results that are not original to this work.

Name Last name: Diba Zare

Signature:

ABSTRACT

APPLICATION OF STIMULI-RESPONSIVE CYSTEINE-BASED ORGANOGELS AS A DRUG DELIVERY SYSTEM FOR CHEMOTHERAPY DRUGS

Zare, Diba
Master of Science, Biotechnology
Supervisor: Assoc. Prof. Dr. Salih Özçubukçu
Co-Supervisor: Assoc. Prof. Dr. Emrullah Görkem Günbaş

August 2023, 55 pages

Cancer is one of the deadliest diseases and researchers are trying to replace chemotherapy as an aggressive treatment with safer treatments for instance immunotherapy. Chemotherapy is the main clinical treatment for malignancies, even though most chemotherapeutic medicines, including doxorubicin, have poor water solubility, resulting in low bioavailability and significant side effects. There has been much research into identifying and developing stimulus-sensitive agents to deliver chemotherapeutic medications to the target area and release therapeutic quantities of these drugs in the cancer area safely and efficiently. For the past few decades, stimuli-responsive organogels grabbed more attention as a potential drug delivery system for chemotherapy drugs.

Cysteine derivatives having disulfide bonds (-S-S-) in their side chain can be used as stimuli-responsive organogelators as the disulfide bond can be cleaved in the presence of certain reducing agents such as thiol derivatives like tris (2-carboxyethyl) phosphine hydrochloride (TCEP), beta-mercaptoethanol (BME), dithiothreitol (DTT), and glutathione (GSH). Glutathione is a tripeptide that consists of cysteine, glutamic acid, and glycine. Studies show that cells of certain cancers have higher levels of glutathione due to increased production of reactive oxygen species (ROS). Some of the classical tumor promoters also activate GSH synthesis

and turnover mechanisms. This feature allows targeted cancer therapy using glutathione-responsive drug delivery systems.

This thesis studied the drug delivery property of cysteine-based organogelators like L-Cys(*t*-dodecyl-sulfanyl)-OH and L-Cys-(S*t*Bu)-OH with a disulfide bond in their side chain that can be cleaved in the presence of glutathione. the organogels were prepared using sunflower oil as the nonpolar solvent and doxorubicin was used as the chemotherapy drug. The drug release property of these organogels was measured in the presence of different concentrations of GSH and was compared with the drug release property of L-Cys-(*t*Bu)-OH based organogel which does not contain a disulfide bond in its side chain in sunflower oil as the negative control group. Furthermore, the biocompatibility of the organogelators was measured in vitro using the L929 cell line and the characterization of the organogels was measured using TEM imaging, XRD, and Rheological measurements.

The results indicated that both L-Cys(*t*-dodecyl-sulfanyl)-OH and L-Cys-(S*t*Bu)-OH can form organogels in sunflower oil and can release doxorubicin in the presence of GSH. Also, the characterization studies confirmed their gel form criteria. Moreover, the in vitro biocompatibility studies did not show significant toxicity to the L929 cells for all the concentrations of L-Cys-(S*t*Bu)-OH and low concentrations of L-Cys(*t*-dodecyl-sulfanyl)-OH.

Keywords: drug delivery systems, doxorubicin, low molecular weight organogelator, glutathione

ÖZ

KEMOTERAPİ İLAÇLARINA İLAÇ TAŞIMA SİSTEMİ OLARAK UYARANLARA YANITLI SİSTEİN BAZLI ORGANOJELLERİN UYGULANMASI

Zare, Diba
Yüksek Lisans, Biyoteknoloji
Tez Yöneticisi: Doç. Dr. Salih Özçubukçu
Ortak Tez Yöneticisi: Doç. Dr. Emrullah Görkem Günbaş

Ağustos 2023, 55 sayfa

Kanser en ölümcül hastalıklardan biridir ve araştırmacılar agresif bir tedavi olarak kemoterapiyi daha güvenli tedavilerle, örneğin immünoterapiyle değiştirmeye çalışıyorlar. Doksorubisin de dahil olmak üzere çoğu kemoterapötik ilacın suda çözünürlüğü zayıf olmasına ve bunun sonucunda düşük biyoyararlanım ve önemli yan etkilere neden olmasına rağmen, maligniteler için ana klinik tedavi kemoterapidir. Kemoterapötik ilaçları hedef bölgeye ulaştırmak ve bu ilaçların terapötik miktarlarını kanser bölgesine güvenli ve verimli bir şekilde salmak için uyarana duyarlı ajanların belirlenmesi ve geliştirilmesine yönelik çok sayıda araştırma yapılmıştır. Son birkaç on yılda, uyaranlara duyarlı organojeller, kemoterapi ilaçları için potansiyel bir ilaç salinim sistemi olarak daha fazla dikkat çekti.

Yan zincirlerinde disülfür bağları (-S-S-) bulunan sistein türevleri, tris (2-karboksietil) fosfin hidroklorür (TCEP), beta-merkaptoetanol (BME), ditiyotreitol (DTT) ve glutatyon (GSH). Glutatyon, sistein, glutamik asit ve glisinden oluşan bir tripeptittir. Çalışmalar, belirli kanser hücrelerinin, reaktif oksijen türlerinin (ROS)

artan üretimi nedeniyle daha yüksek glutatyon seviyelerine sahip olduğunu göstermektedir. Klasik tümör promotörlerinden bazıları ayrıca GSH sentezini ve dönüşüm mekanizmalarını da aktive eder. Bu özellik, glutatyona yanıt veren ilaç dağıtım sistemleri kullanılarak hedeflenen kanser tedavisine izin verir.

Bu tez, L-Cys(*t*-dodesil-sülfanil)-OH ve L-Cys-(S*t*Bu)-OH gibi sistein bazlı organojelatörlerin, yan zincirlerinde parçalanabilen bir disülfür bağı ile ilaç verme özelliğini inceleyecektir. Organojeller polar olmayan çözücü olarak ayçiçek yağı kullanılarak hazırlandı ve kemoterapi ilacı olarak doksorubisin kullanıldı. Farklı GSH konsantrasyonları varlığında ilaç salım özellikleri ölçüldü ve yan zincirinde disülfür bağı içermediği için negatif kontrol grubu olarak ayçiçek yağındaki L-Cys-(*t*Bu)-OH bazlı organojel ile karşılaştırıldı. Ayrıca, organojelatörlerin biyouyumluluğu in vitro olarak ölçüldü ve organojellerin karakterizasyonu, TEM görüntüleme, XRD ve reolojik ölçümler kullanılarak ölçüldü.

Sonuçlar, hem L-Cys(*t*-dodesil-sülfanil)-OH hem de L-Cys-(S*t*Bu)-OH'nin ayçiçek yağında organojel oluşturabildiğini ve GSH varlığında doksorubisin salabildiğini gösterdi. Ayrıca, karakterizasyon çalışmaları jel formu kriterlerini doğrulamıştır. Ayrıca in vitro biyouyumluluk çalışmaları, L-Cys-(S*t*Bu)-OH'nin tüm konsantrasyonları ve düşük L-Cys(*t*-dodesil-sülfanil)-OH konsantrasyonları için L929 hücrelerine önemli bir toksisite göstermedi.

Anahtar Kelimeler: ilaç taşıyıcı sistemler, doksorubisin, düşük molekül ağırlıklı organojel, Glutatyon

To my father, mother, and sister;

who with effort and love have accompanied me in this process,

without hesitating at any moment to see my dreams come true.

ACKNOWLEDGMENTS

At this point, I can easily see how many individuals have supported me to reach this achievement. I want to use this opportunity to express my sincere thanks to everyone who helped me over these years.

I would like to convey my profound thanks to my supervisor and co-supervisor, Assoc. Prof. Dr. Salih Özçubukçu and Assoc. Prof. Dr. Emrullah Görkem Günbaş, for their unconditional guidance, inspiration, encouragement, and words of motivation throughout the duration of my research to ensure the completion of this work. Their expertise, availability to discuss ideas, and willingness to give their knowledge were crucial.

I gratefully thank Dr. Aytül Saylam, Dr. Güzide Aykent, Dr. Zübeyir Elmazoglu, Dr. Melek Parlak Khalily, Batuhan Baytekin, and Gamze Yılmaz for their constructive help and comments to improve the quality of this thesis. I also thank Assoc. Prof. Dr. Ferdi Karadaş from Bilkent University for the XRD measurements.

Collective and individual acknowledgments are owed to my labmates; Elif Akar, Dilay Kepil, Mehmet Seçkin Kesici, Volkan Dolgun, Berat Koçaş, Enes Uzun, Yalçın Boztaş, Medine Soydan, and Yağmur Tanış whose presence was perpetually refreshed, helpful, and memorable.

Finally, I would like to convey my heartiest thanks to my parents and my sister for their support and love during my stay in Turkey.

Diba Zare

TABLE OF CONTENTS

LIST OF TABLES

LIST OF FIGURES

LIST OF SCHEMES

LIST OF ABBREVIATIONS

ORG: Organogel

LMWO: low molecular weight organogelator

LMWG: Low molecular weight gelator

GSH: Glutathione

ROS: Reactive oxygen species

DOX: Doxorubicin

TEM: Transmission electron microscopy

XRD: X-ray diffraction analysis

HRMS: High-resolution mass spectrometry

NMR: Nuclear magnetic resonance spectroscopy

TLC: Thin layer chromatography

Fmoc: Fluorenylmethyloxycarbonyl

PBS: Phosphate-buffered saline

TIPS: Triisopropyl silane

DCM: Dichloromethane

THF: Tetrahydrofuran

TFA: Trifluoroacetic acid

NCS: N-chloro-succinimide

DMEM: Dulbecco's modified eagle medium

MeOD: Deuterated methanol

$CDCl_3$: Deuterated chloroform

***d_6*-DMSO:** Deuterated dimethyl sulfoxide

CHAPTER 1

INTRODUCTION

1.1 Drug delivery of chemotherapeutic drugs by organogels

Cancer is one of the deadliest diseases and researchers are trying to replace chemotherapy as an aggressive treatment with safer treatments for instance immunotherapy, meanwhile, every year a large number of anticancer medications gain rapid approval and chemotherapy is the main clinical treatment for malignancies even though most chemotherapeutic medicines, including doxorubicin, have poor water solubility, resulting in low bioavailability and significant side effects. Furthermore, according to the biopharmaceutics classification system, approximately 40% of worldwide approved drugs are poorly water-soluble [1-3]. Various methods are used to increase solubility and bioavailability of chemotherapeutic drugs and among them, lipid-based formulations have shown promising results for the improvement of active ingredient bioavailability.

Lipid-based formulations have been extensively used to immobilize and carry drugs [4], vaccines [5], antigens [6], proteins [7], microbial cells [8], and animal cells [9]. The pharmaceutical industries usually employed lipid-based formulations to increase the active ingredient loading capacity, stability, and bioavailability of medications by allowing active ingredients to be transported by lipid carriers. In general, vegetable oils are frequently employed as lipid carriers and can be obtained from plant sources [10]. Vegetable oil-based formulations can be used for controlled-release applications in the dosage forms of liquid, semi-solid, or solid which are known as emulsions, organogels, and microparticles, respectively.

Transporting and releasing chemotherapeutic drugs to the target area (tissues or cells) safely and efficiently, are the main challenges facing the development of

chemotherapeutic agents. There has been much research into identifying and designing stimulus-sensitive agents for transporting and releasing chemotherapeutic drugs to the cancer area and for the past few decades, stimuli-responsive organogels grabbed more attention as a potential drug delivery system for chemotherapy drugs.

1.2 Organogels (ORGs)

A gel is a soft solid that contains both solid and liquid components where the solid component, known as the gelator, is present as a network of aggregates that immobilize the liquid component and prevents the it from flowing [11]. In general, gels have been divided into two categories depending on the polarity of the liquid component; hydrogels, which are prepared in polar solvents like water, and organogels, which are prepared in nonpolar solvents like organic liquids, vegetable oils, etc [12].

Organogels are semi-solid formulations which comprise a three-dimensional network structure of gelator molecules and an immobilized nonpolar liquid. Organogels have been investigated as drug delivery formulation in pharmaceutical applications and their use has been increasing, which may be correlated to their long-term stability, ease of preparation, and cost-effectiveness [13]. Although hydrogels have a high market value because of their patient compliance nature as they can be easily washed with water because of their non-oily nature, they have limited ability to accommodate a variety of drugs and cross the lipophilic barriers. Since organogels can easily transport both hydrophilic and lipophilic pharmaceuticals through lipophilic barriers and can be used as vehicles for drug delivery applications, these drawbacks of hydrogels have been addressed by using organogels.

Organogels have been synthesized using different gelators such as low molecular weight organogelators (LMWOs) with organic non-polar solvents. These low molecular weight gelators (LMWGs) are based on organic compounds with less than 2 kDa molecular weights. If they self-assemble into gels in organic solvents or oils,

they are organogelators, if they self-assemble into gels in ionic liquids, they are ionogelators [14], and if they assemble into gels in water, they are hydrogelators. During the formation of organogels, the gelator molecules form a 3-D structure either by chemical cross-linking like covalent and ionic bonds, or physical entanglement like hydrogen bonds, Van der Waal forces, and π-π interactions to immobilize the non-polar liquid component [15].

The immobilization of the solvent is caused by the entanglement of the secondary structures leading to organogel formation [16-18]. The important factor for gelation is the interactions and packing between organagelator molecules [19]. The size and shape of the 3-D structures depend on the gelator-solvent interactions. The properties of organogels are dependent on the structuring ability of the organogelators and the properties of the incorporated compounds such as drugs or bioactive formulations. A list of the organogelators which were used in the pharmaceutical applications is shown in Table 1. The molecular packing of the organogels may be characterized by transmission electron microscopy (TEM) and X-ray diffraction analysis (XRD) [20].

Table 1: List of organogelators used in pharmaceutical applications.

Organogelator	Reference
2,3-didecycloxytetracene	[21]
Cholesteryl 4-(2-anthryloxy) butanoate	[22]
Diacid monoamides of cholesteryl glycinate ammonium salts	[23]
Palladium pincer bis (carbene) complex	[24]
Cholesteryl L-phenyl alaninate	[25]
Cholic acid amino-alkylamides	[26]

Bis (N-lauroyl-L-lysine ethyl ester) oxyl amide	[27]
L-alanine derivative and phenylalanine derivatives of N-protected phthaloylhydrazide amino acids, L-tyrosine derivatives	[28-30]
Lecithin, spans, tweens phytosterols+oryzanol compounds, stearic acid, and its derivatives	[31,32]
Derivatives of methyl glycosides of 4,6-O-benzylidine	[33]
Polyethylene	[34]

1.3 Amino acids and their LMWO derivatives

Amino acids are versatile chemicals for self-assembled structures, and in the form of low molecular weight organogelators, they have a wide range of use such as drug delivery, smart electronics, and stimuli-responsive materials. Low molecular weight organogels have gained substantial scientific attention during the last two decades [35-39].

Amino acids are biocompatible and can easily be further modified at the carboxyl or amine moieties and turn into numerous LMWG. Especially, for the last twenty years, low molecular weight organogels are used in many applications in drug delivery systems, tissue engineering, and electronic applications [13, 36, 38, 40]. In the drug delivery side of organogels, for instance, L-alanine and L-tyrosine derivatives were turned into a safflower oil-based gel as an injectable organogel which was used in the rivastigmine, an acetylcholinesterase inhibitor for the Alzheimer treatment, drug delivery [30]. Although various types of organogels are made, there are few studies on the use of organogels in medicine due to low biocompatibility and high toxicity of organic solvents that are present in organogels. To minimize organogels toxicity, amino acids and their derivatives can be used to form self-assembly and gel via

hydrogen bonds and Van der Waal forces. The presence of different functional units on the side chains of amino acids and their protecting groups may affect the gel formation positively. For instance, L-Tyr(*t*Bu)-OH (Figure 1) acts as a low molecular weight organogelator in a wide range of organic solvents [29].

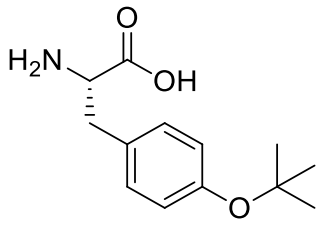

Figure 1: Chemical structure of L-Tyr(*t*Bu)-OH

1.4 Stimuli-responsive gels

Once a gel forms, changes in pH, redox environment, temperature, or exposure to certain enzymes or agents can lead to gel disruption, and this phenomenon has been used in drug release studies [41]. The gel-solution transition can be stimulated by changing the physical or chemical conditions. Generally, heat, mechanical forces, ultrasonic waves, and UV-vis lightare known as the physical external stimuli, meanwhile, pH, redox, and enzyme reagents are known as the chemical stimulus [42]. These properties give the amino acid-based gelators the potential to be used in different applications such as drug delivery, dye removal, oil-spill recovery, etc [43]. Stimuli-responsive drug delivery systems enable the delivery of payloads on-demand, at a specific time, and a specific location [44].

1.4.1 Temperature-responsive gels

Any imbalance in the body's temperature or pH can alter the immune response and cause infectious diseases, autoimmune disorders, and cancer. Thus, pH and thermo-responsive carriers are considered as the next generation of drug delivery systems, which are able to release drugs intelligently in response to external or internal stimuli

[45]. For instance, increasing temperature leads to a gel-solution phase transition and the gelation temperature is the temperature at which the gel turns into solution [46].

1.4.2 Mechanical-responsive gels

One of the most important properties of gels is their viscoelastic properties, thus, most of the physical gel systems are responsive to mechanical stress and application of a mechanical force can deform or destroy the gel depending on the amount of applied force. Also, some gels are thixotropic which means the gel state is restored when the stress is removed [47].

1.4.3 Ultrasound-induced gels

If a gel cannot be formed by heating or cooling process, the gelation process may occur under an ultrasound condition. Sometimes, even microwave irradiation or vigorous shaking are not able to form gels [48]. Ultrasound possesses several advantages as a stimulus for drug delivery platforms as it allows controlling the material properties and functions easily and safely. It is non-invasive, non-ionizing, and localized, leading to a deep tissue penetration, focused and localized to a small region of interest, and spatiotemporal control. Using ultrasound in stimuli-responsive gels happens by transferring energy to induce a response.

1.4.4 Light-responsive gels

Light is one of the best ways to use as stimuli because it is clean, fast, and controllable, and because of that photo responsive gels have gotten lots of attention in the last decade. Photochemical reactions can adjust the gel properties after the light beam [49]. In the light-responsive gels, the solvent-to-gel or gel-to-solvent phase transition of the gel system can be controlled by light-induced trans−cis

isomerization of the gel units. the gel which is formed from the trans isomer can turn into the solvent when the trans-to-cis isomerization of the units is induced photochemically, and this phase-transition process can be repeated reversibly [50].

1.4.5 Redox-responsive gels

The redox stimulus is important when dealing with artificial muscles, electromechanical soft materials, and drug release for various diseases. Functional groups that can undergo oxidation-reduction reactions have been associated with LMWOs to make the gel respond to the redox environment [51].

Drug carriers containing disulfide bonds have been extensively studied because they are reductively cleavable in intracellular environments by the action of glutathione (GSH), a typical biological reducing agent [52]. For instance, novel cubic gel particles (ssCGP) were synthesized and operated in triggered drug release by using the biodegradable disulfide bond-bearing feature and glutathione [53].

To maintain a highly reducing environment or enhanced oxidative stress, tumor cells are known to overproduce intracellular glutathione (GSH) or reactive oxygen species (ROS). Overproduced GSH and ROS might exist in distinct tumors, various locations within the same tumor, or at different periods of tumor growth, which is intriguing. GSH/ROS-responsive targeted drug release has been suggested to be an appealing technique for discovering anti-tumor medicines as a result of this. The design and synthesis of intelligent biopolymer systems have been triggered by the thiolysis of the disulfide bond by GSH or the oxidation of the thioether to hydrophilic sulfoxide [54].

1.5 Glutathione

Glutathione (GSH) is a tripeptide consisting of glutamate, cysteine, and glycine and the most abundant low molecular weight peptide in eukaryotic cells (Figure 2). It is

a reducing agent that maintains enzymes in an active state. Its function has been recognized and showed that changes in GSH levels have been associated with cancer, AIDS, aging, liver diseases heart attack, etc. Higher levels of GSH are observed around several types of cancer or tumor cells, allowing using GSH-responsive agents targeted drug release. Intercellular GSH concentration can be used to trigger disulfide thiol exchange and drug release by reducing the disulfide bond of the drug-loaded gels [55-57].

ROS production is enhanced in cancer cells that trigger an adaptive response by increasing GSH levels and activating GSH-dependent enzymes. Moreover, the enzymes involved in GSH synthesis, such as GCL, GR, GPX, and GST, are overexpressed in several cancers [58].

Studies show that in the cells of certain cancer types, there are higher glutathione levels compared to the others. For instance, the HeLa cell line, an immortal cervical cancer cell line, has more glutathione levels in comparison with the 4T1 cell line, an epithelial breast cancer derived from the mammary gland tissue of BALB/c mice. Both HeLa and 4T1 cell lines have more GSH levels compared to the L929 cell line, a mouse fibroblast cell line, which is a normal cell line [59-61].

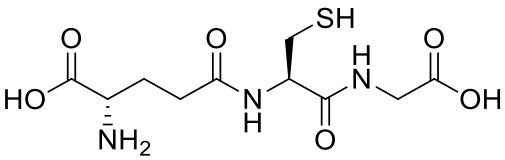

Figure 2: Chemical structure of glutathione.

1.6 Doxorubicin

Doxorubicin, shown in Figure 3, is a chemotherapy drug in the anthracycline and antitumor antibiotic family of medications [62]. It has been routinely used in the treatment of several cancers including breast cancer, bladder cancer, Kaposi's sarcoma, lymphoma, and acute lymphocytic leukemia. There are two proposed mechanisms by which doxorubicin acts in the cancer cell: intercalation into DNA

and disruption of topoisomerase-II-mediated DNA repair and generation of free radicals and their damage to cellular membranes and proteins. In brief, doxorubicin is oxidized to semiquinone, an unstable metabolite, which is converted back to doxorubicin in a process that releases reactive oxygen species. Reactive oxygen species can lead to lipid peroxidation and membrane damage, DNA damage, oxidative stress, and triggers apoptotic pathways of cell death [63]. Common side effects of doxorubicin include hair loss, bone marrow suppression, vomiting, rash, and inflammation of the mouth.

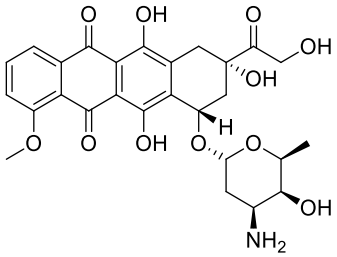

Figure 3: Chemical structure of doxorubicin.

1.7 Research objectives

According to the literature, different amino acid derivatives have been analyzed for gelation properties. L-Tyr(*t*Bu)-OH with a proper side chain unit was able to form a self-assembled gel with π-π and Van der Waals interactions [29]. Keeping all the points that were mentioned in mind, we hypothesized that cysteine derivatives having disulfide bonds in the side chain can be used as a stimuli-responsive organogelator and the disulfide bond can be cleaved in the presence of GSH. This feature allows targeted cancer therapy using glutathione-responsive drug delivery systems by the organogels form changing from gel to solution state (Figure 4).

This thesis studied the drug release property of L-Cys(S*t*Bu)-OH and L-Cys(*t*-dodecyl-sulfanyl)-OH based organogels with a disulfide bond in their side chain in comparison with L-Cys(*t*Bu)-OH based organogel without the disulfide bond in its side chain in presence of GSH. Organogels were prepared using a non-essential oil

such as sunflower oil as the nonpolar organic solvent and doxorubicin was used as a chemotherapy drug. Morphological characterization of the obtained organogels was also carried out.

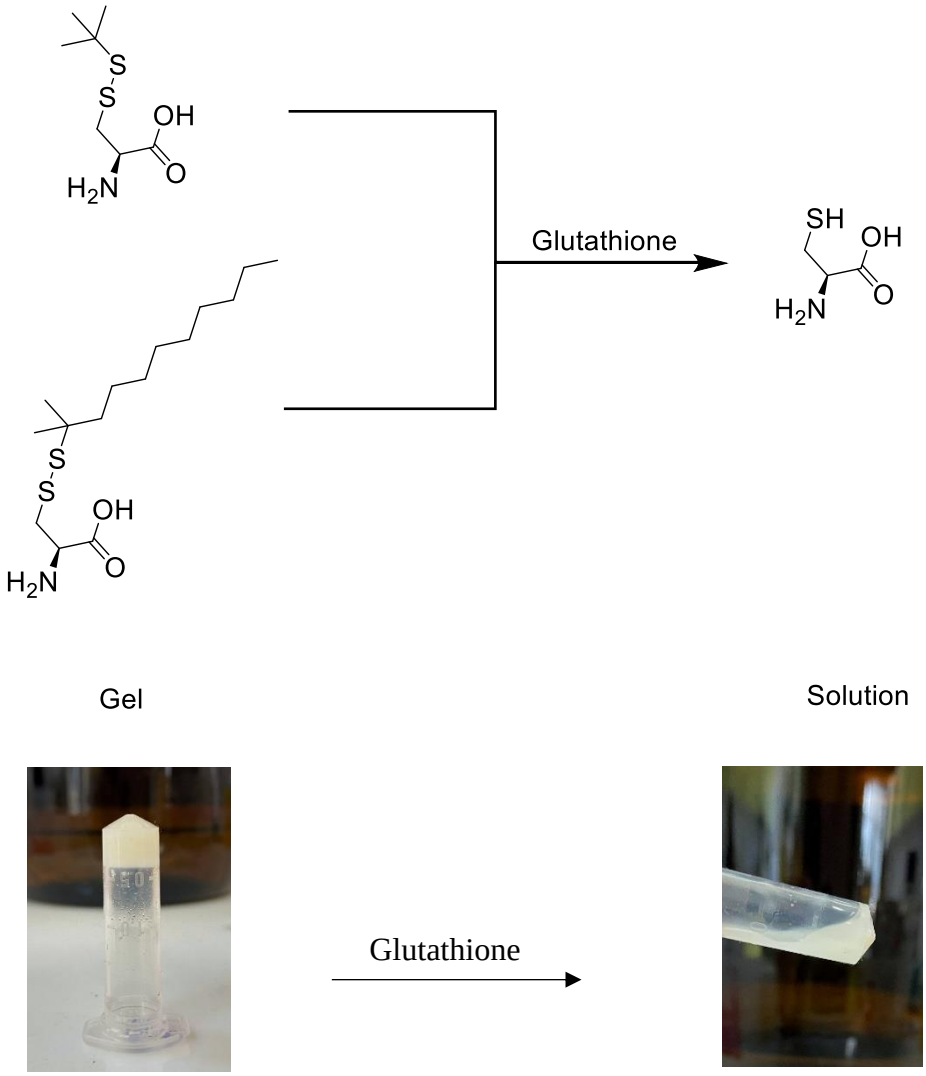

Figure 4: Organogels form changing from gel to solution state in the presence of glutathione.

CHAPTER 2

RESULTS AND DISCUSSION

2.1 Synthesis of Fmoc-L-Cys-OH

Fmoc-L-Cys-OH was synthesized using Fmoc-L-Cys(Trt)-OH. 5 g Fmoc-L-Cys(Trt)-OH was dissolved in 340 mL DCM and its trityl group was removed using 40 mL trifluoroacetic acid (TFA) for 10 minutes in room temperature. 10 mL triisopropylsilane (TIPS) was added to the solution to form a stable adduct with the trityl by-product and prevents it from reacting with the substrate (Scheme 1) [64]. The yield was 97%.

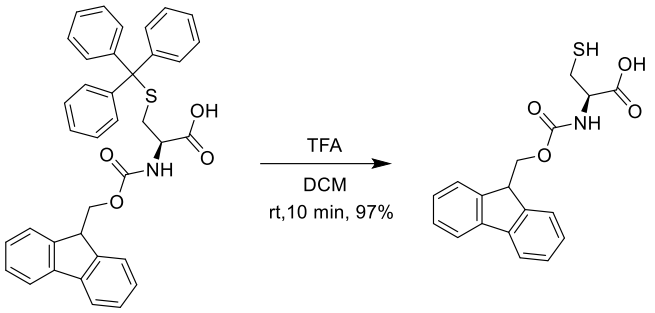

Scheme 1: Synthesis of Fmoc-L-Cys-OH.

2.2 Synthesis of Fmoc-L-Cys(*t*-dodecyl-sulfanyl)-OH

Fmoc-L-Cys(*t*-dodecyl-sulfanyl)-OH was synthesized by adding 2.4 g NCS (N-chlorosuccinimide) to 4.1 mL *tert*-dodecanethiol in 66 mL DCM at -78 ℃ and the mixture stirred for 45 minutes to bond the Cl in NCS to the sulfur atom in *tert*-dodecanethiol increasing the reactivity of the molecule in further reactions. The mixture of NCS and *tert*-dodecanethiol in DCM was poured into a stirring solution

of 3 g Fmoc-L-Cys-OH in 75 mL THF at -78 ℃ and stirred for 5 hours (Scheme 2). All the reactions were cooled to -78 °C in a dry ice-acetone bath. Reaction mixture was then washed with 5% hydrochloric acid in water and the organic layer was collected over $MgSO_4$, filtered, and evaporated under reduced pressure. The crude was then purified using silica gel column chromatography [65]. The yield was 46%.

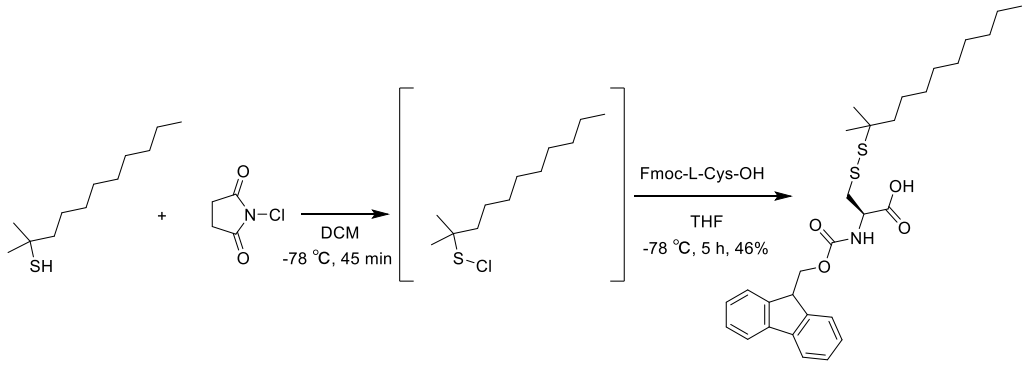

Scheme 2: Synthesis of Fmoc-L-Cys(*t*-dodecyl-sulfanyl)-OH.

2.3 Synthesis of L-Cys(S*t*Bu)-OH

L-Cys(S*t*Bu)-OH was synthesized using Fmoc-L-Cys(S*t*Bu)-OH. 0.47 g Fmoc-L-Cys(S*t*Bu)-OH was dissolved in 8 mL THF and the Fmoc protecting groups was removed by adding 0.5 mL piperidine to the mixture and it was stirred at room temperature overnight (Scheme 3). Piperidine forms a stable adduct with the dibenzofulvene by-product and prevents it from reacting with the substrate. The yield was 97%.

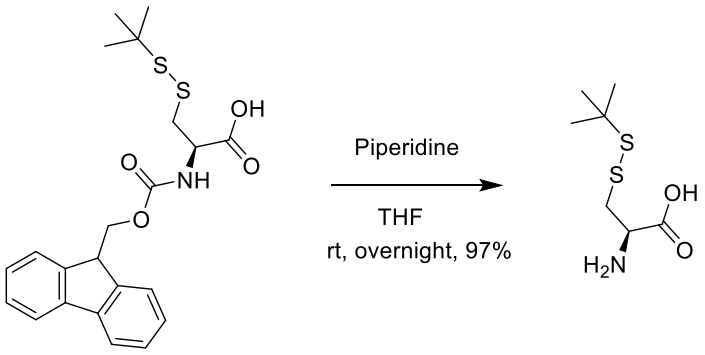

Scheme 3: Synthesis of L-Cys(S*t*Bu)-OH.

2.4 Synthesis of L-Cys(*t*Bu)-OH

L-Cys(*t*Bu)-OH was synthesised using Fmoc-L-Cys(*t*Bu)-OH. 0.44 g Fmoc-L-Cys(*t*Bu)-OH was dissolved in 8 mL THF and the Fmoc protecting groups was removed by adding 0.5 mL piperidine to the mixture and it was stirred at room temperature overnight (Scheme 4). Piperidine forms a stable adduct with the dibenzofulvene by-product and prevents it from reacting with the substrate. The yield was 98%.

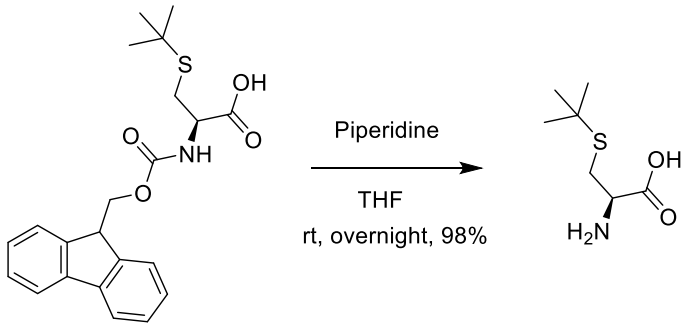

Scheme 4: Synthesis of L-Cys(*t*Bu)-OH.

2.5 Synthesis of L-Cys(*t*-dodecyl-sulfanyl)-OH

L-Cys(*t*-dodecyl-sulfanyl)-OH was synthesised using Fmoc-L-Cys(*t*-dodecyl-sulfanyl)-OH. 1.2 g Fmoc-L-Cys(*t*-dodecyl-sulfanyl)-OH was dissolved in 16 mL THF and the Fmoc protecting groups was removed by adding 1 mL piperidine to the mixture and it was stirred at room temperature overnight (Scheme 5). Piperidine forms a stable adduct with the dibenzofulvene by-product and prevents it from reacting with the substrate. The yield was 68%.

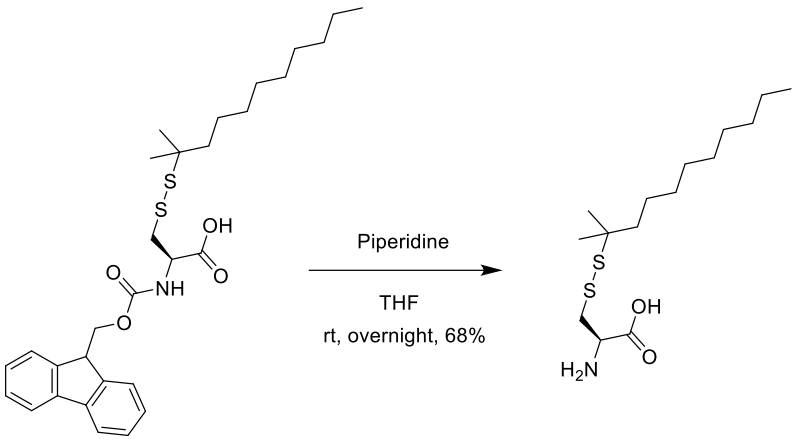

Scheme 5: Synthesis of L-Cys(*t*-dodecyl-sulfanyl)-OH.

2.6 Preparation of organogels

Generally, for preparing organogels, a specific amount of the gelator which can immobilize the non-polar solvent, should be dissolved in an organic solvent like sunflower oil, followed by sonication in the sonic bath. Depending on the organogelator and mobile phase, the sonication time, temperature, and probability of adding base can be different.

2.6.1 Preparation of L-Cys(S*t*Bu)-OH based organogel

The gelation properties of L-Cys(S*t*Bu)-OH are shown in Table 2 and Figure 5 using different wt/v% of L-Cys(S*t*Bu)-OH in sunflower oil. The L-Cys(S*t*Bu)-OH was dissolved in sunflower oil followed by 20 minutes ultrasonic bath at 35 °C.

Table 2: wt/v% amounts of L-Cys(S*t*Bu)-OH used for gel formation in sunflower oil.

Cysteine derivative	wt/v %	Sunflower oil	Cysteine derivative weight	Result
L-Cys(S*t*Bu)-OH	3%	0.25 mL	7.5 mg	solution
L-Cys(S*t*Bu)-OH	4%	0.25 mL	10 mg	solution
L-Cys(S*t*Bu)-OH	5%	0.25 mL	12.5 mg	gel
L-Cys(S*t*Bu)-OH	6%	0.25 mL	15 mg	gel
L-Cys(S*t*Bu)-OH	7%	0.25 mL	17.5 mg	gel
L-Cys(S*t*Bu)-OH	8%	0.25 mL	20 mg	gel

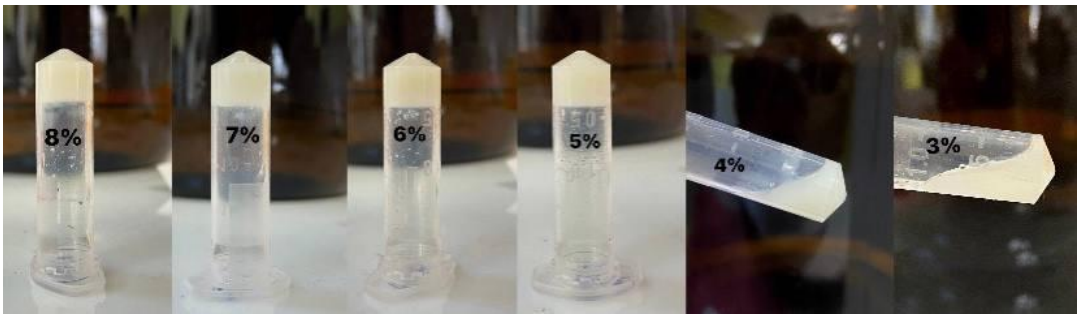

Figure 5: 3, 4, 5, 6, 7, and 8 wt/v% L-Cys(S*t*Bu)-OH based organogels in sunflower oil.

The gelation properties of L-Cys(S*t*Bu)-OH are shown in Table 3 and Figure 6 by adding of 10 M NaOH as the base. Different wt/v% of the L-Cys(S*t*Bu)-OH was dissolved in sunflower oil followed by adding 10 M NaOH then 10 minutes ultrasonic bath at 35 °C. the results indicated that adding 10 M NaOH as the base to L-Cys(S*t*Bu)-OH based gels can decrease the gelation percentage to 1%.

Table 3: Different amounts of 10 M NaOH used for L-Cys(S*t*Bu)-OH based gel formation in sunflower oil.

Cysteine derivative	wt/v %	Sunflower oil	Cysteine derivative weight	Base (10 M NaOH)	Result
L-Cys(S*t*Bu)-OH	4%	0.25 mL	10 mg	10 µL	gel
L-Cys(S*t*Bu)-OH	3%	0.25 mL	7.5 mg	10 µL	gel
L-Cys(S*t*Bu)-OH	2%	0.25 mL	5 mg	10 µL	gel
L-Cys(S*t*Bu)-OH	1%	0.25 mL	2.5 mg	10 µL	gel

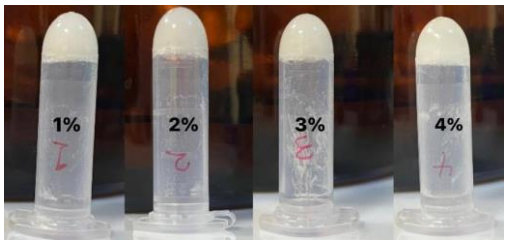

Figure 6: Different amounts of 10 M NaOH used for L-Cys(S*t*Bu)-OH based gel formation in sunflower oil.

2.6.2 Preparation of L-Cys(*t*Bu)-OH based organogel

The gelation properties of L-Cys(*t*Bu)-OH are shown in Table 4 and Figure 7 using different wt/v% of L-Cys(*t*Bu)-OH in sunflower oil. The L-Cys(*t*Bu)-OH was dissolved in sunflower oil followed by 20 minutes ultrasonic bath at 35 °C.

Table 4: wt/v% amounts of L-Cys(*t*Bu)-OH used for gel formation in sunflower oil.

Cysteine derivative	wt/v %	Sunflower oil	Cysteine derivative weight	Result
L-Cys(*t*Bu)-OH	3%	0.25 mL	7.5 mg	solution
L-Cys(*t*Bu)-OH	4%	0.25 mL	10 mg	solution
L-Cys(*t*Bu)-OH	5%	0.25 mL	12.5 mg	solution
L-Cys(*t*Bu)-OH	6%	0.25 mL	15 mg	gel

Figure 7: 6 wt/v% L-Cys(*t*Bu)-OH based organogel in sunflower oil.

2.6.3 Preparation of L-Cys(*t*-dodecyl-sulfanyl)-OH based organogel

The gelation properties of L-Cys(*t*-dodecyl-sulfanyl)-OH are shown in Table 5 and Figure 8 with different amounts of 10 M NaOH as the base and in Table 6 and Figure 9 using different wt/v% of L-Cys(*t*-dodecyl-sulfanyl)-OH in sunflower oil. The L-Cys(*t*-dodecyl-sulfanyl)-OH was dissolved in sunflower oil followed by adding 10 M NaOH then 10 minutes ultrasonic bath at 45 °C.

Table 5: Different amounts of 10 M NaOH used for L-Cys(*t*-dodecyl-sulfanyl)-OH based gel formation in sunflower oil.

Cysteine derivative	wt/v %	Sunflower oil	Cysteine derivative weight	Base (10 M NaOH)	Result
L-Cys(*t*-dodecyl-sulfanyl)-OH	5%	0.15 mL	7.5 mg	2.5 µL	solution
L-Cys(*t*-dodecyl-sulfanyl)-OH	5%	0.15 mL	7.5 mg	5 µL	solution
L-Cys(*t*-dodecyl-sulfanyl)-OH	5%	0.15 mL	7.5 mg	8.5 µL	solution
L-Cys(*t*-dodecyl-sulfanyl)-OH	5%	0.15 mL	7.5 mg	10 µL	gel

Figure 8: 2.5, 5, 8.5, and 10 µL of 10 M NaOH used for 5 wt/v% L-Cys(*t*-dodecyl-sulfanyl)-OH based gel formation in sunflower oil.

Table 6: wt/v% amounts of L-Cys(*t*-dodecyl-sulfanyl)-OH used for gel formation in sunflower oil.

Cysteine derivative	wt/v %	Sunflower oil	Cysteine derivative weight	Base (10 M NaOH)	Result
L-Cys(*t*-dodecyl-sulfanyl)-OH	0%	0.15 mL	0.0 mg	10 µL	solution
L-Cys(*t*-dodecyl-sulfanyl)-OH	0.5%	0.15 mL	0.75 mg	10 µL	gel
L-Cys(*t*-dodecyl-sulfanyl)-OH	1%	0.15 mL	1.5 mg	10 µL	gel
L-Cys(*t*-dodecyl-sulfanyl)-OH	2%	0.15 mL	3.0 mg	10 µL	gel
L-Cys(*t*-dodecyl-sulfanyl)-OH	3%	0.15 mL	4.5 mg	10 µL	gel
L-Cys(*t*-dodecyl-sulfanyl)-OH	4%	0.15 mL	6.0 mg	10 µL	gel
L-Cys(*t*-dodecyl-sulfanyl)-OH	5%	0.15 mL	7.5 mg	10 µL	gel

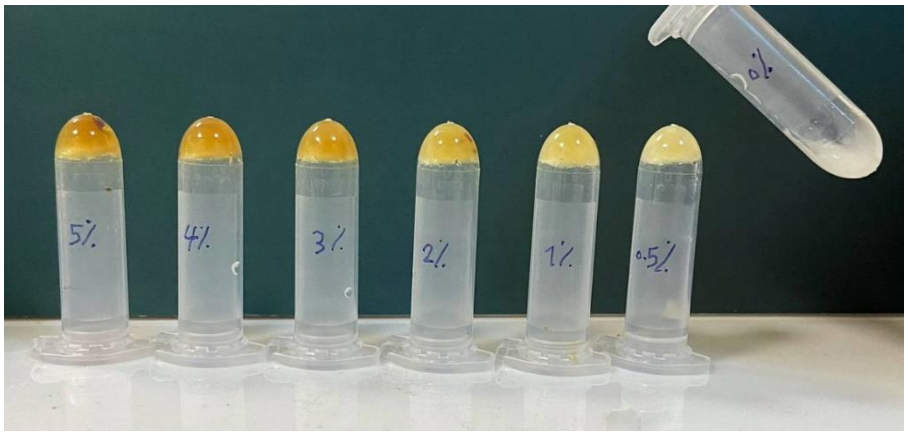

Figure 9: 0, 0.5, 1, 2, 3, 4, and 5 wt/v% L-Cys(*t*-dodecyl-sulfanyl)-OH based organogels in sunflower oil.

2.7 Organogels characterization

The characterization of the microstructures, molecular packing at an atomic scale, and viscosity properties of organogels were performed using the transmission electron microscope (TEM) imaging, X-ray powder diffraction (XRD) measurements, and Rheometer, respectively.

2.7.1 Transmission electron microscopy (TEM) imaging

The TEM images of 5 wt/v% L-Cys(S*t*Bu)-OH in THF and 5 wt/v% L-Cys(*t*-dodecyl-sulfanyl)-OH in sunflower oil based organogels are shown in Figure 10 and 11, respectively. The TEM images of both L-Cys(S*t*Bu)-OH and L-Cys(*t*-dodecyl-sulfanyl)-OH based organogels show the formation of nano-fibers with an approximate width of 20 nm and a varied micrometers length.

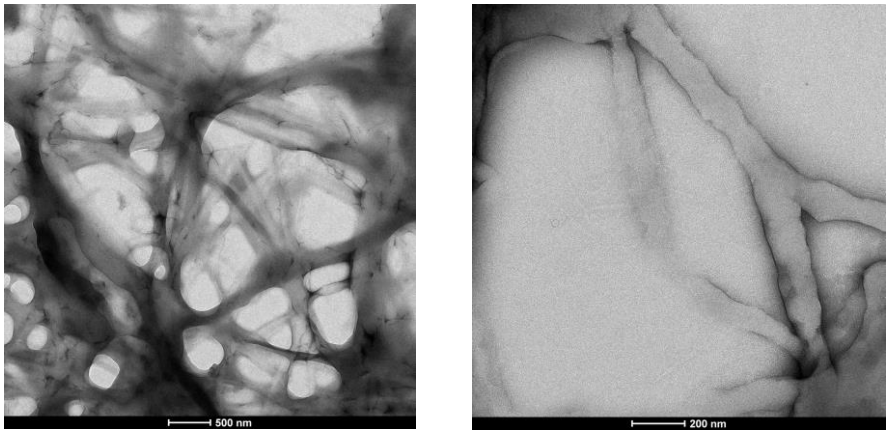

Figure 10: TEM images of 5 wt/v% L-Cys(S*t*Bu)-OH based organogel in THF.

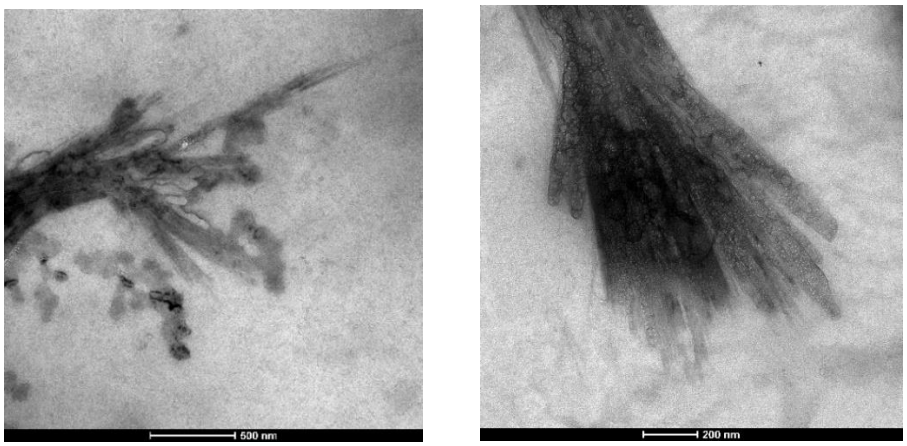

Figure 11: TEM images of 5 wt/v% L-Cys(*t*-dodecyl-sulfanyl)-OH based organogel in sunflower oil.

2.7.2 X-ray diffraction analysis (XRD) measurements

The physicochemical nature of the formulations was studied by X-ray diffraction (XRD) measurement to show the morphology of the formulations in their native state. Figures 12 and 13 show the L-Cys(S*t*Bu)-OH based organogel structure and its XRD measurement where the d1 represent the Van der Waals interactions distance and d2 represents the hydrogen bonds distance of this organogel. Figures 14 and 15 show the L-Cys(*t*-dodecyl-sulfanyl)-OH based organogel structure and its XRD measurement where the d1 represent the Van der Waals interactions distance and d2 represents the hydrogen bonds distance of this organogel.

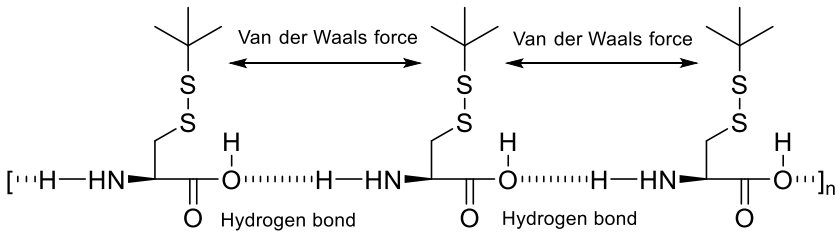

Figure 12: L-Cys(S*t*Bu)-OH based organogel structure.

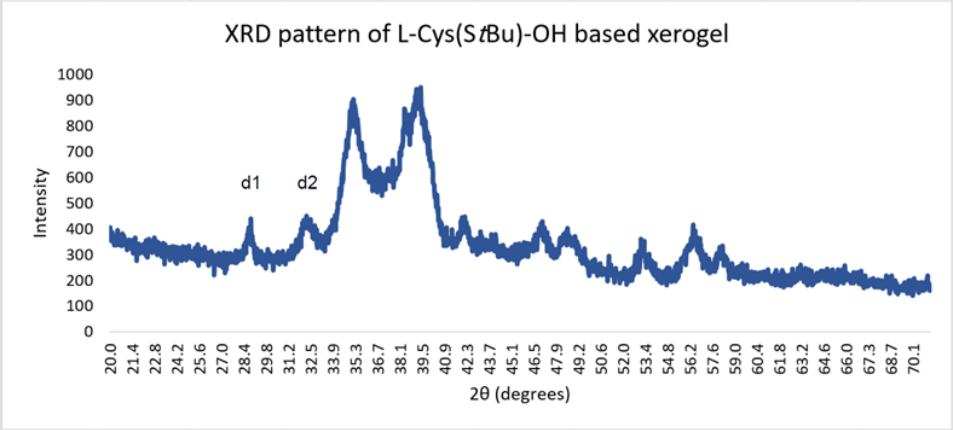

Figure 13: XRD pattern of L-Cys(S*t*Bu)-OH based organogel in THF; d1= 3.183 Å and 2θ = 28.95°, d2 = 2.886 Å and 2θ = 32.26°.

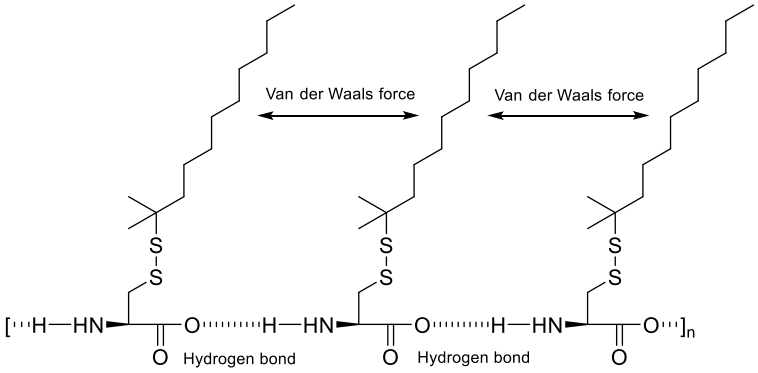

Figure 14: L-Cys(*t*-dodecyl-sulfanyl)-OH based organogel structure.

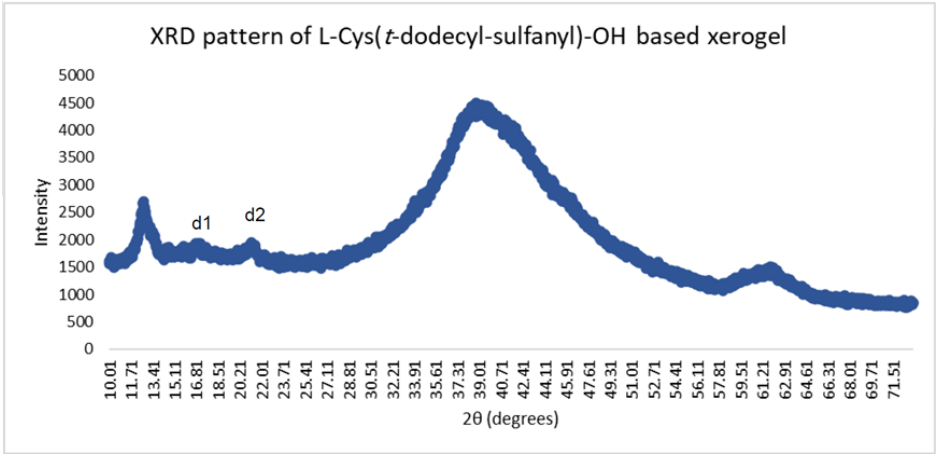

Figure 15: XRD pattern of L-Cys(*t*-dodecyl-sulfanyl)-OH based organogel in sunflower oil; d1 = 5.222 Å and 2θ = 17.15°, d2 = 4.268 Å and 2θ = 21.14°.

2.7.3 Rheological measurements

Gelation kinetics was determined by a time-sweep test within the linear viscoelastic range. Time sweep tests of of the 5 wt/v% L-Cys(S*t*Bu)-OH and L-Cys(*t*-dodecyl-sulfanyl)-OH based organogels in sunflower were carried until storage and loss modulus reached plateau. Storage modulus (G′) and loss modulus (G″) were monitored under a strain sweep of 0.01−500% at a frequency of 10 rad/s at 25 °C. For both of the organogels, storage modulus (G′) were greater than loss modulus (G″) confirming the gel character of the resulting networks. The L-Cys(S*t*Bu)-OH based organogel rheological graph represents a gel form (Figure 16) and the L-Cys(*t*-dodecyl-sulfanyl)-OH based organogel rheological graph represents a paste-gel form (Figure 17).

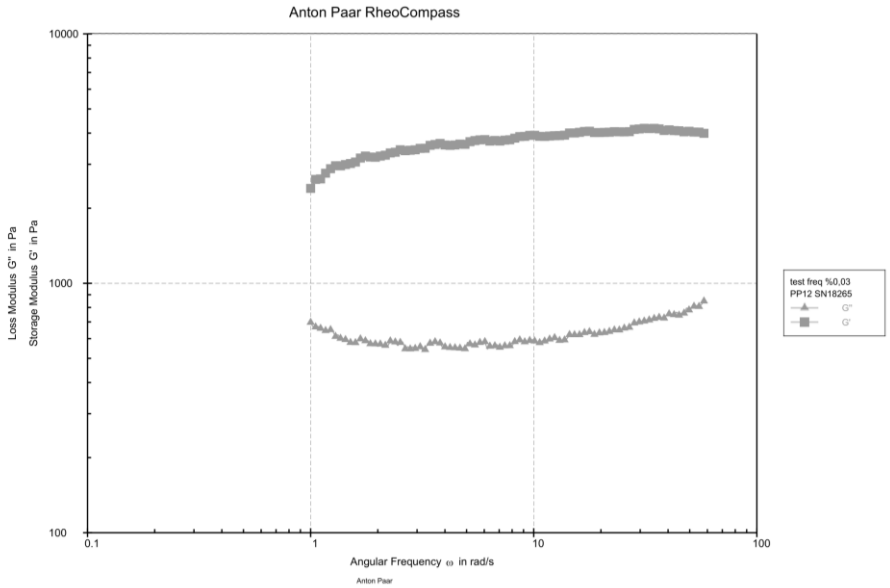

Figure 16: Time-sweep test of 5 wt/v% L-Cys(S*t*Bu)-OH based organogel in sunflower oil.

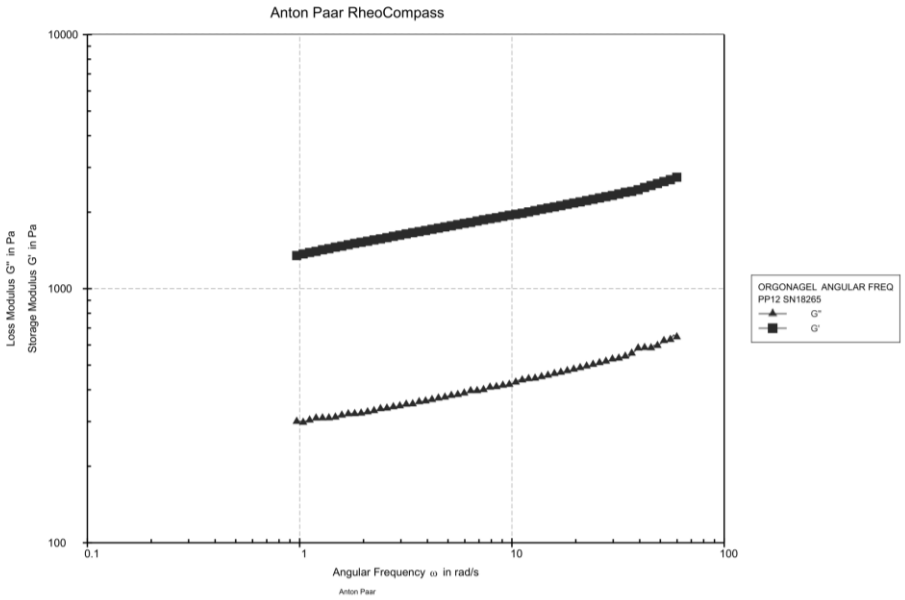

Figure 17: Time-sweep test of 5 wt/v% L-Cys(*t*-dodecyl-sulfanyl)-OH based organogel in sunflower oil.

2.7.4 Drug release kinetics of the organogels

2.7.4.1 Drug release kinetics of DOX loaded 6 wt/v% L-Cys(S*t*Bu)-OH based organogel

In this study, we investigated the releasing time and amount of DOX from 6 wt/v% L-Cys(S*t*Bu)-OH based organogel network. The 6 wt/v% L-Cys(*t*Bu)-OH based organogel was used as a negative control group as it does not contain a disulfide bond in its side chain. The DOX loaded organogels were prepared by adding 60 µL of the 0.006 g doxorubicin in 1.2 mL propylene glycol solution into 0.015 g of organogelators (L-Cys(S*t*Bu)-OH and L-Cys(*t*Bu)-OH) and 0.25 mL sunflower oil in Eppendorf tubes. The organogels were formed using a 35 °C sonic bath for 20 minutes and then they were stirred overnight.

Organogels were divided into two groups; EXP1 and EXP2. In EXP1, 0.025 g GSH was added into 30 mL release buffer with pH 7.2 to trigger disruption of the network

by cleaving disulfide bond. In EXP2, 0.075 g GSH was added into 30 mL release buffer with pH 7.2 to trigger disruption of the network by cleaving disulfide bond. 1 mL of the GSH-PBS solution was added on the top of the gels for EXP1 and EXP2.

As it is shown in Figure 18, the DOX loaded 6 wt/v% L-Cys(S*t*Bu)-OH based organogel lost its gel form and turned into the solution in the presence of GSH by cleaving the disulfide bond in its side chain and the DOX was released into the PBS solution on the top of the organogel. Meanwhile, the DOX-loaded 6 wt/v% L-Cys(*t*Bu)-OH based organogel remained in the gel form and the GSH could not affect the organogel as there is no disulfide bond in this molecule to be cleaved and cause solution formation.

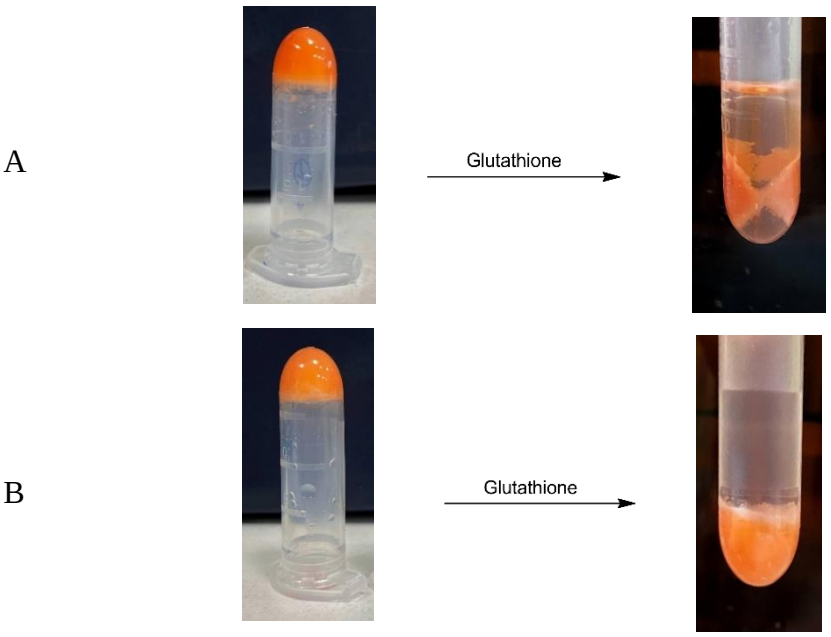

Figure 18: (A) L-Cys(S*t*Bu)-OH and (B) L-Cys(*t*Bu)-OH DOX loaded organogels drug release in the presence of GSH.

As the drug release kinetic graphs shows (Figures 19 and 20), the final amount of drug released in DOX loaded 6 wt/v% L-Cys(S*t*Bu)-OH based organogels in the presence of higher concentrations of GSH (EXP2) were approximately double than lower concentrations of GSH (EXP1) and both of the groups drug releases were more than DOX loaded 6 wt/v% L-Cys(*t*Bu)-OH based organogels. Moreover, the higher

concentration of GSH (EXP2) did not affect DOX loaded 6 wt/v% L-Cys(*t*Bu)-OH based organogels drug release.

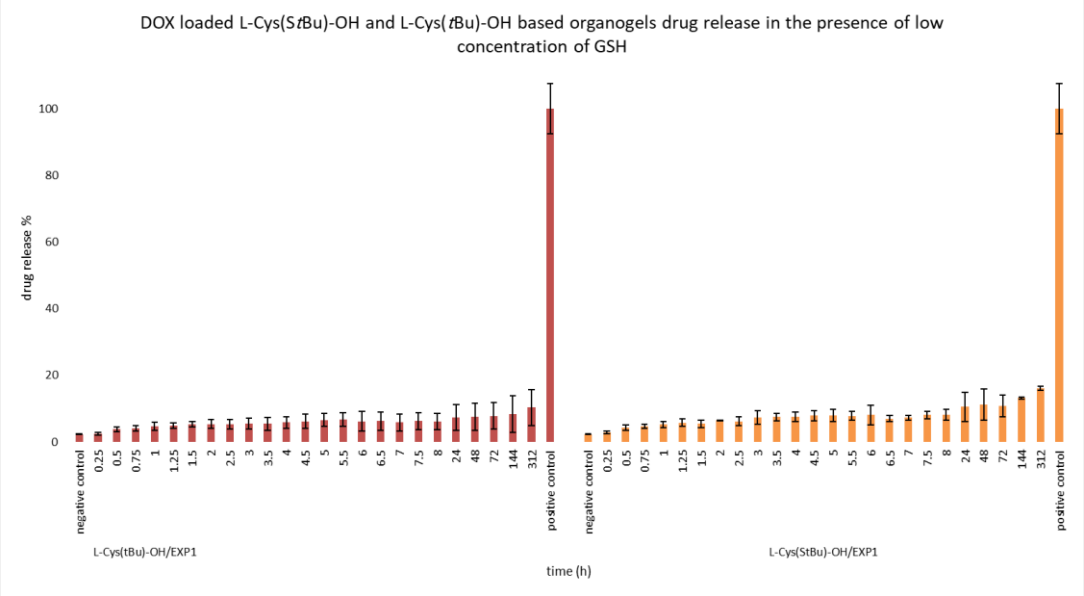

Figure 19: Drug release kinetics of DOX loaded L-Cys(S*t*Bu)-OH and L-Cys(*t*Bu)-OH organogels in the presence of a low concentration of GSH (0.025 g GSH in 30 mL PBS).

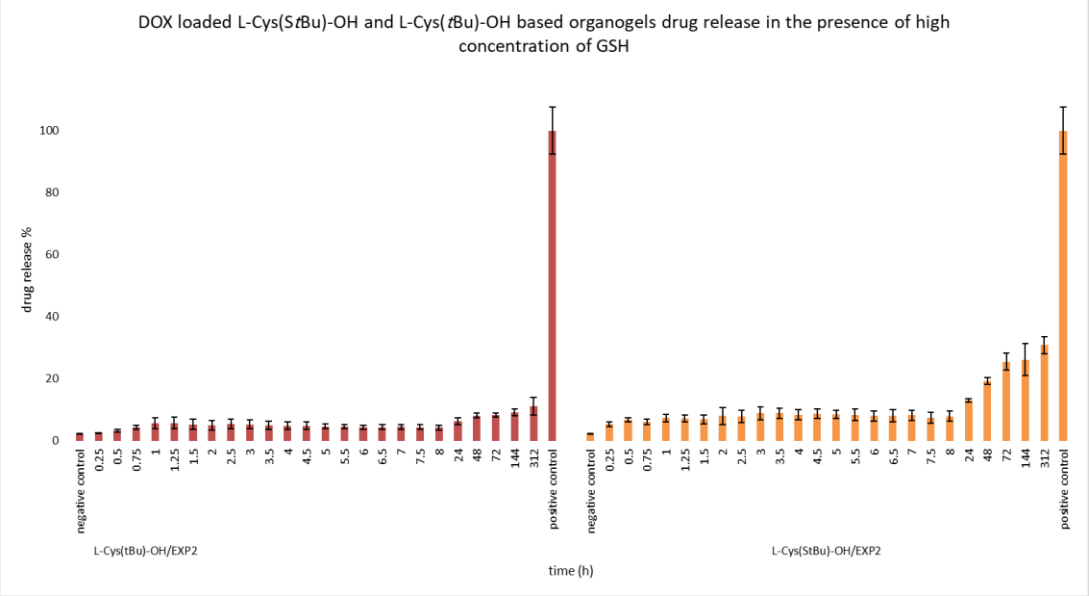

Figure 20: Drug release kinetics of DOX loaded L-Cys(S*t*Bu)-OH and L-Cys(*t*Bu)-OH organogels in the presence of a high concentration of GSH (0.075 g GSH in 30 mL PBS).

2.7.4.2 Drug release kinetics of the DOX loaded 6 wt/v% L-Cys(*t*-dodecyl-sulfanyl)-OH based organogel

In this study, we investigated the releasing time and amount of DOX from 6 wt/v% L-Cys(*t*-dodecyl-sulfanyl)-OH based organogel network. The 6 wt/v% L-Cys(*t*Bu)-OH based organogel was used as a negative control group as it does not contain a disulfide bond in its side chain. The organogels were perepared by adding 13 µL 10 M NaOH to 0.012 g of organogelators (L-Cys(*t*-dodecyl-sulfanyl)-OH and L-Cys(*t*Bu)-OH) in 0.2 mL sunflower oil in Eppendorf tubes. The organogels were formed using a 45 °C sonic bath for 10 minutes for L-Cys(*t*-dodecyl-sulfanyl)-OH based organogels and 35 °C sonic bath for 1 minute for L-Cys(*t*Bu)-OH based organogels. The organogels stirred overnight at room temperature. The day after, 10 µL of the 0.006 g doxorubicin in 0.2 mL propylene glycol solution was injected in the middle of the gels and stirred overnight.

Organogels were divided into two groups; EXP1 and EXP2. For EXP1, 0.025 g GSH was added into 30 mL release buffer with pH 7.2 to trigger disruption of the network by cleaving disulfide bond. For EXP2, 0.075 g GSH was added into 30 mL release buffer with pH 7.2 to trigger disruption of the network by cleaving disulfide bond. 1 mL of the GSH-PBS solution was added on the top of the gels for EXP1 and EXP2.

As it is shown in Figure 21, the DOX-loaded 6 wt/v% L-Cys(*t*-dodecyl-sulfanyl)-OH based organogel lost its gel form and turned into the solution in the presence of GSH by cleaving the disulfide bond in its side chain and the DOX was released into the PBS solution on the top of the organogel. Meanwhile, the DOX-loaded 6 wt/v% L-Cys(*t*Bu)-OH based organogel remained in the gel form and the GSH could not affect the organogel as there is no disulfide bond in this molecule to be cleaved and cause solution formation.

A

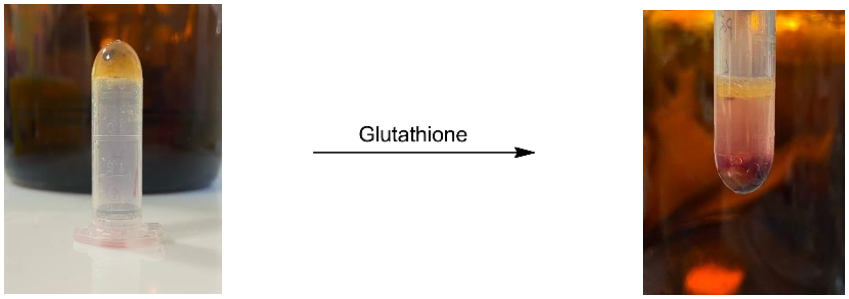

B

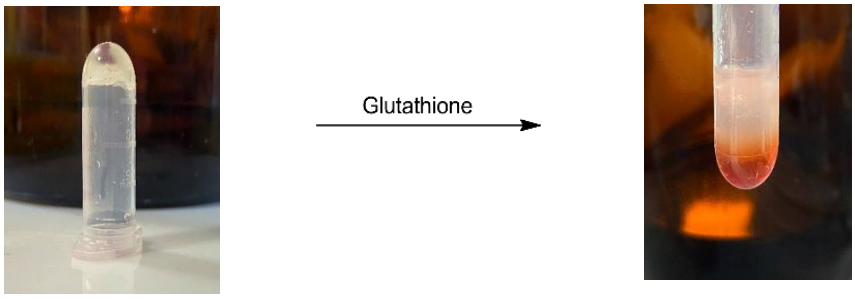

Figure 21: (A) L-Cys(*t*-dodecyl-sulfanyl)-OH and (B) L-Cys(*t*Bu)-OH DOX loaded organogels drug release in the presence of GSH.

As the drug release kinetic graphs shows (Figures 22 and 23), the amount of drug released in DOX loaded 6 wt/v% L-Cys(*t*-dodecyl-sulfanyl)-OH based organogels in the presence of higher concentrations of GSH (EXP2) reached the highest DOX release concentration 11 days earlier than the lower concentrations of GSH (EXP1) and both of the groups drug releases was approximately 3.5 times more than DOX loaded 6 wt/v% L-Cys(*t*Bu)-OH based organogels. Moreover, the higher concentration of GSH (EXP2) did not affect DOX loaded 6 wt/v% L-Cys(*t*Bu)-OH based organogels drug release.

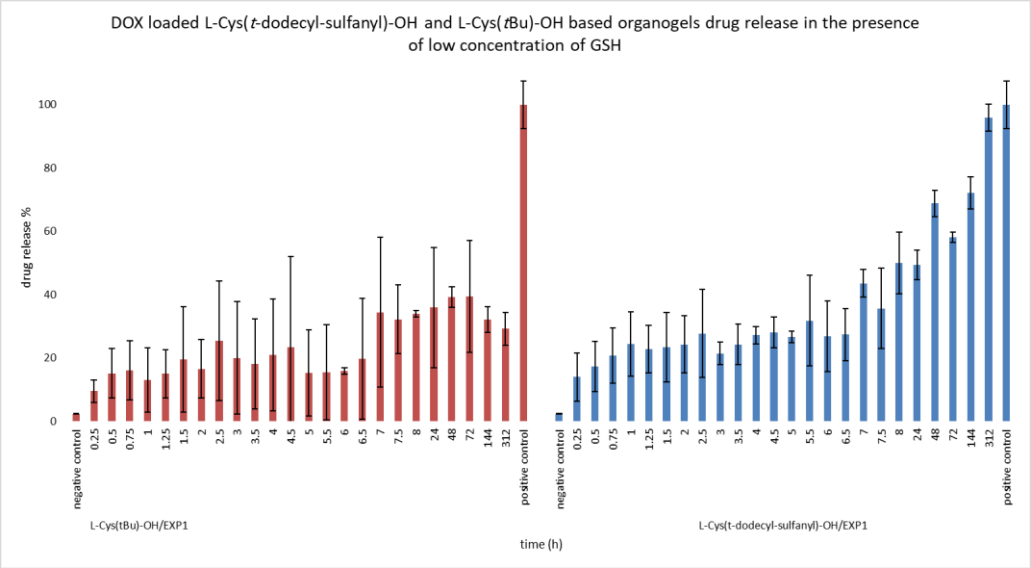

Figure 22: Drug release kinetics of DOX loaded L-Cys(*t*-dodecyl-sulfanyl)-OH and L-Cys(*t*Bu)-OH organogels in the presence of a low concentration of GSH (0.025 g GSH in 30 mL PBS).

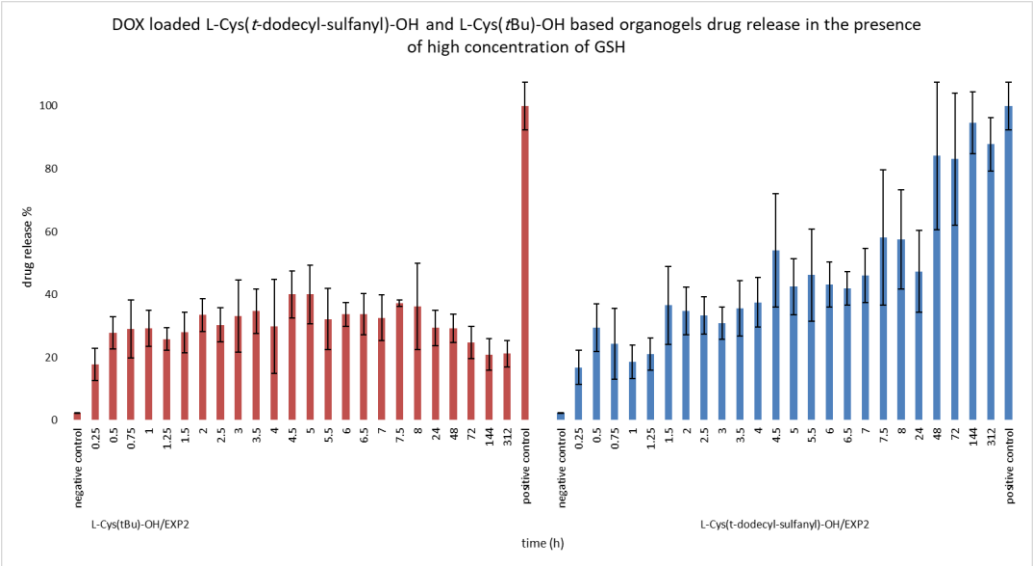

Figure 23: Drug release kinetics of DOX loaded L-Cys(*t*-dodecyl-sulfanyl)-OH and L-Cys(*t*Bu)-OH organogels in the presence of a high concentration of GSH (0.075 g GSH in 30 mL PBS).

2.7.5 In vitro biocompatibility study

In order to measure the toxicity of organogelators, MTT assay was done. L929 cells were treated with different concentrations of L-Cys(*t*-dodecyl-sulfanyl)-OH and L-Cys(S*t*Bu)-OH organogelators and L-Cys-OH was used as a source of amino acid which these organogelators were derived from, for a better comparison of the toxicity of organogelators. The biocompatibility study showed toxicity in 3 highest concentrations of L-Cys(*t*-dodecyl-sulfanyl)-OH organogelator in 24 hand 48 h, meanwhile, in 4 lower concentrations of this organogelator we did not see a considerable toxicity to the cells. L-Cys(S*t*Bu)-OH and L-Cys-OH did not show a considerable toxicity to the cells in any concentrations in 24 h and five lower concentrations in 48 h (Figures 24 and 25).

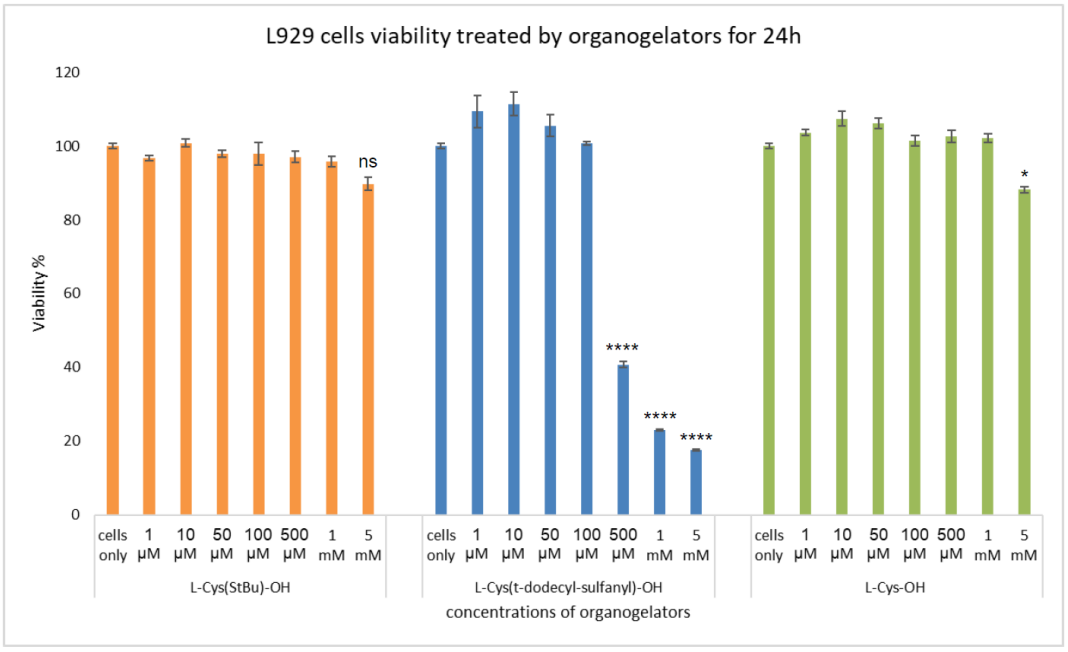

Figure 24: L929 cells viability treated with different concentrations of L-Cys-OH, L-Cys(*t*-dodecyl-sulfanyl)-OH, and L-Cys(S*t*Bu)-OH for 24 h.

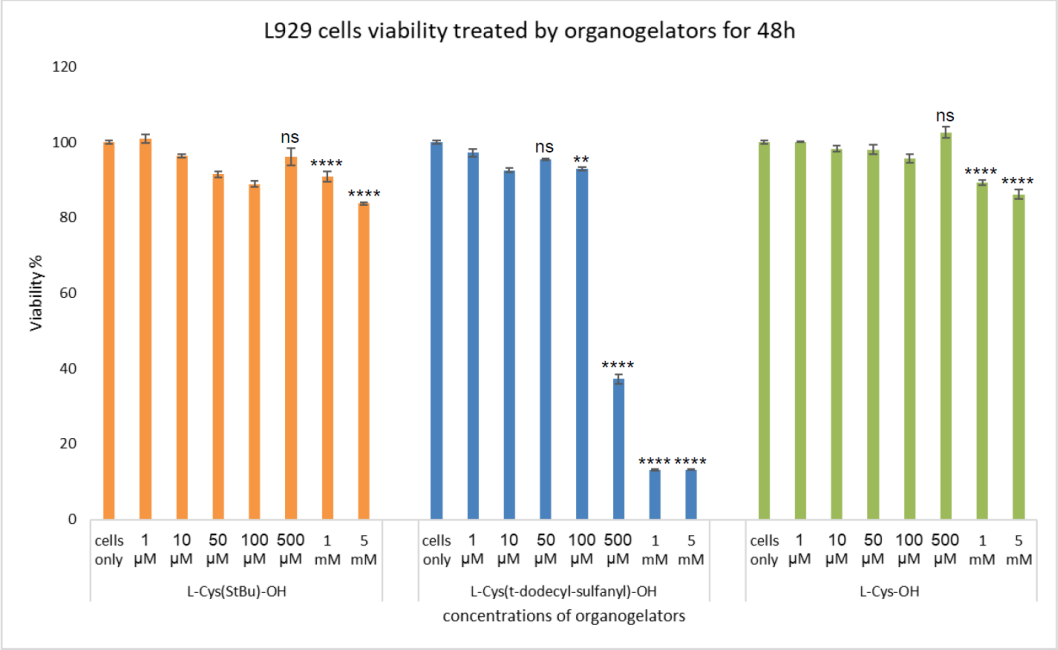

Figure 25: L929 cells viability treated with different concentrations of L-Cys-OH, L-Cys(*t*-dodecyl-sulfanyl)-OH, and L-Cys(S*t*Bu)-OH for 48 h.

2.8 Discussion

In conclusion, the characterization studies confirmed the gel form criteria and microfiber formation in both L-Cys(S*t*Bu)-OH and L-Cys(*t*-dodecyl-sulfanyl)-OH based organogels and the a time-sweep test showed that L-Cys(S*t*Bu)-OH made a stiffer gel than L-Cys(*t*-dodecyl-sulfanyl)-OH. Although we expected the L-Cys(*t*-dodecyl-sulfanyl)-OH to make a stiffer gel because of the possible stronger Wan der Waals interactions between its long side chains, but as the *tert*-dodecanthiol that was used in this study was a mixture of isomers, so the difference in the molecular structure of L-Cys(*t*-dodecyl-sulfanyl)-OH molecules prevented the formation of strong Wan der Waals interactions. Also, we had to add a base like NaOH to remove the hydrogen atom from L-Cys(*t*-dodecyl-sulfanyl)-OH molecules to boost the hydrogen bond formation between molecules and the temperature at which the L-Cys(*t*-dodecyl-sulfanyl)-OH made gel was higher than the L-Cys(S*t*Bu)-OH.

The drug release studies showed that L-Cys(*t*-dodecyl-sulfanyl)-OH based organogels can release the DOX faster and in a greater amount compared to the L-Cys(S*t*Bu)-OH based organogels which is because of the difference in their structure as the L-Cys(S*t*Bu)-OH based organogels are stiffer than L-Cys(*t*-dodecyl-sulfanyl)-OH based organogels. Also, we saw that the GSH could turn the L-Cys(*t*-dodecyl-sulfanyl)-OH and L-Cys(S*t*Bu)-OH based organogels into solution by cleaving the disulfide bond in their side chain, meanwhile, the GSH did not affect the L-Cys(*t*Bu)-OH based organogel as there is no disulfide bond in its side chain. Furthermore, the higher concentrations of GSH increased the released drug amount in L-Cys(*t*-dodecyl-sulfanyl)-OH and L-Cys(S*t*Bu)-OH based organogels and it did not affect the L-Cys(*t*Bu)-OH based organogel.

Although the in vitro biocompatibility study showed toxicity for higher concentrations of the L-Cys(*t*-dodecyl-sulfanyl)-OH, but because of its great drug release properties it can be still used in lower concentrations for drug delivery systems.

Overall, L-Cys(*t*-dodecyl-sulfanyl)-OH and L-Cys(S*t*Bu)-OH based organogels can be used in chemotherapy drug deliveries in the form of injectable nanoparticles and they can deliver and release the chemotherapy drugs in the cancer area safely. Further in vitro and in vivo studies are needed to confirm their ability as a drug delivery system for this aim.

CHAPTER 3

MATERIAL AND METHOD

3.1 Materials

Fmoc-L-Cys(S*t*Bu)-OH, Fmoc-L-Cys(*t*Bu)-OH, Fmoc-L-Cys(Trt)-OH, and L-Cys-OH.HCL was purchased from Chem-Impex International Inc. L-Glutathione reduced (GSH), phosphate buffered saline (PBS), and triisopropyl silane (TIPS) were purchased from Sigma-Aldrich. Dichloromethane (DCM), tetrahydrofuran (THF), and trifluoroacetic acid (TFA) were purchased from Carlo Erba. Water and hexane were purchased as technical grade and dried over magnesium sulphate ($MgSO_4$) in a distillation system. *Tert*-dodecanethiol, N-chloro-succinimide (NCS), silica gel 60 (0.063-0.20 mm) for purification of organic molecules, and silica gel TLC plates containing F254 fluorescent indicator enabling the visualization at 254 nm for reaction progress monitoring were purchased from Merck Schuchardt. Hydrochloric acid was purchased from Birpa. Diethyl ether (Et_2O) and methanol purchased from ISOLAB. 1,2-propandiol purchased from Schuchardt München. Uranyl acetate was purchased from Fisher. DMEM purchased from Serana. Piperidine was purchased from Thermo Scientific. Sunflower oil was purchased from Yudum. UV measurements were applied via the BioTek microplate reader instrument. TEM imaging measurements were applied via FEI Tecnai G2 Spirit BioTwin CTEM. HRMS measurements were applied in positive and negative mode (ES+/ES-) in the range of 50 – 1000 Da (ESI-TOF-MS) with Waters SYNAPT G1 MS instrument. Rheology measurements were applied using Physica MCR 301, Anton Paar Rheometer. The XRD measurements were done using X'Pert³ MRD with Cu Kα X-ray radiation ($\lambda = 1.5406$ Å).

3.2 Synthesis of Fmoc-L-Cys-OH

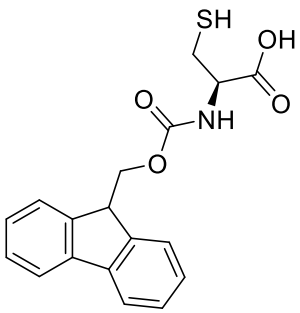

Based on the literature procedure [64], 5.00 g (8.54 mmol) Fmoc-L-Cys(Trt)-OH was dissolved in 340 mL DCM followed by adding 10 mL (48.8 mmol) triisopropylsilane (TIPS) and 40 mL (0.52 mol) trifluoroacetic acid (TFA), respectively. The reaction mixture was stirred for 10 minutes at room temperature until the orange solution turned colorless. The reaction mixture was concentrated under reduced pressure using Et_2O as the co-evaporated for removing TFA. The residue was suspended in hexane and centrifuged followed by discarding the supernatant and the pellet was resuspended in hexane (cycle was repeated 5 times) to remove the trityl amino protecting group. The pellet was dried under reduced pressure. 2.85 g (8.3 mmol) of white solid was obtained and the yield was 97%. TLC (DCM: MeOH = 10: 1).

^{1}H NMR (400 MHz, DMSO) δ 7.90 (d, *J* = 7.5 Hz, 2H), 7.74 (dd, *J* = 8.0, 3.7 Hz, 2H), 7.42 (t, *J* = 7.4 Hz, 2H), 7.34 (t, *J* = 7.4 Hz, 2H), 4.31 (d, *J* = 6.2 Hz, 2H), 4.25 (q, *J* = 7.6 Hz, 1H), 4.12 (td, *J* = 8.4, 4.3 Hz, 1H), 2.89 (ddd, *J* = 13.0, 8.4, 4.3 Hz, 1H), 2.73 (dt, *J* = 13.6, 8.5 Hz, 1H).

3.3 Synthesis of Fmoc-L-Cys(*t*-dodecyl-sulfanyl)-OH

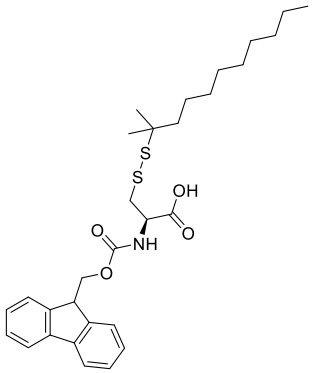

Based on the literature procedure [65], 2.4 g (18 mmol) NCS (N-chlorosuccinimide) was dissolved in 66 mL DCM at -78 °C and stirred at the same temperature for 20 minutes followed by adding 4.10 mL (17.4 mmol) *tert*-dodecanethiol. The reaction was stirred at -78 °C temperature for another 45 minutes. The mixture was quickly poured into a stirring solution of 3.00 g (8.7 mmol) Fmoc-L-Cys-OH in 75 mL THF at -78 °C. The whole mixture was stirred for the

next 5 hours maintaining the temperature at -78 ℃. The reaction was then allowed to come to room temperature (25 ℃). The reaction mixture was then washed with acidified water (5% hydrochloric acid in water) 3 times. The organic layer was collected over $MgSO_4$, filtered, and evaporated under reduced pressure. The crude was then purified using silica gel column chromatography, using DCM: MeOH (10: 0.5) as a mobile phase. 2.16 g (3.96 mmol) of dark yellow viscose material was obtained and the yield was 46%. TLC (DCM: MeOH = 10: 0.5).

^{1}H NMR (400 MHz, $CDCl_3$) δ 7.69 (d, *J* = 7.6 Hz, 2H), 7.55 (d, *J* = 7.4 Hz, 2H), 7.37 – 7.29 (m, 2H), 7.24 (t, *J* = 7.5 Hz, 2H), 4.75 – 4.03 (m, 4H), 3.41 – 2.97 (m, 2H), 1.31 – 0.70 (m, 25H).

^{13}C NMR (101 MHz, $CDCl_3$) δ 174.9, 156.0, 143.6, 143.2, 141.2, 127.5, 127.0, 125.1, 119.9, 67.4, 53.8, 46.9, 30.8, 29.6, 29.4, 27.4, 22.6, 14.3, 14.0, 12.1, 8.7, 0.9.

HRMS $C_{30}H_{41}NO_4S_2$ $[M+Na]^{+:}$ Calculated 543.2477, found 543.2476.

3.4 Synthesis of L-Cys(S*t*Bu)-OH

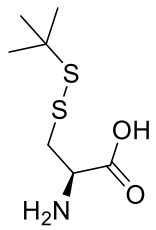

0.47 g (1.1 mmol) Fmoc-L-Cys(S*t*Bu)-OH was dissolved in 8 mL THF and 0.5 mL piperidine and was stirred overnight at room temperature and then concentrated under reduced pressure followed by washing with hexane using a filter paper until the complete removal of the Fmoc protecting group. 0.22 g (1.07 mmol) of white solid was obtained and the yield was 97%. TLC (DCM: MeOH = 10: 1)

^{1}H NMR (400 MHz, MeOD) δ 3.73 (dd, *J* = 10.0, 3.4 Hz, 1H), 3.29 (dd, *J* = 14.2, 3.4 Hz, 1H), 2.86 (dd, *J* = 14.2, 10.1 Hz, 1H), 1.28 (s, 9H).

3.5 Synthesis of L-Cys(*t*Bu)-OH

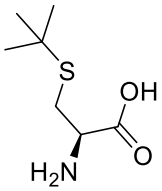

0.44 g (1.1 mmol) Fmoc-L-Cys(*t*Bu)-OH was dissolved in 8 mL THF and 0.5 mL piperidine and was stirred overnight at room temperature and then concentrated under reduced pressure followed by washing with hexane using a filter paper until the complete removal of the Fmoc protecting group. 0.19 g (1.08 mmol) of white solid was obtained and the yield was 98%. TLC (DCM: MeOH = 10: 1)

^{1}H NMR (400 MHz, MeOD) δ 3.53 (dt, *J* = 9.7, 3.7 Hz, 1H), 3.14 (dd, *J* = 13.7, 3.6 Hz, 1H), 2.78 (dd, *J* = 13.7, 9.7 Hz, 1H), 1.27 (s, 9H).

3.6 Synthesis of L-Cys(*t*-dodecyl-sulfanyl)-OH

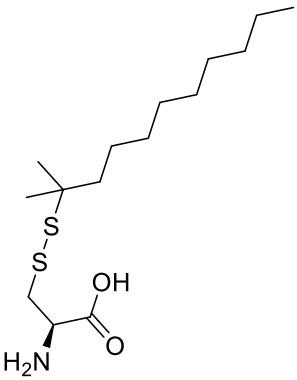

1.20 g (2.2 mmol) Fmoc-L-Cys(*t*-dodecyl-sulfanyl)-OH in 16 mL THF and 1 mL piperidine was stirred overnight at room temperature and then concentrated under reduced pressure. The residue was suspended in hexane and centrifuged followed by discarding the supernatant and the pellet was resuspended in hexane (cycle repeated 5 times) to remove the Fmoc protecting group. The pellet was dried under reduced pressure. 0.48 g (1.5 mmol) of dark brown viscose material was obtained, and the yield was 68%. TLC (DCM: MeOH = 10: 1)

^{1}H NMR (400 MHz, $CDCl_3$) δ 3.67 (s, 1H), 3.06 (s, 2H), 1.18 (m, 25H).

^{13}C NMR (101 MHz, $CDCl_3$) δ 183.8, 68.1, 63.6, 50.5, 44.5, 31.9, 29.7, 22.5, 22.4, 14.1, 1.0.

HRMS $C_{15}H_{31}NO_2S_2$ $[M+H]^+$: calculated 321.1796, found 321.1651.

3.7 Preparation of organogels

3.7.1 Preparation of L-Cys(S*t*Bu)-OH based organogel

To prepare different percentages of organogels from 3 to 8 wt/v% for the L-Cys(S*t*Bu)-OH based organogels, different weights of L-Cys(S*t*Bu)-OH were dissolved in 0.25 mL sunflower oil in an Eppendorf tube and were put in an ultrasonic bath 35 °C for 20 minutes and gel formation occurred spontaneously. If the 10 M NaOH was added as the base, the sonication time was decreased to 1 minute. To test the gel formation, an inversion test was used [29].

3.7.2 Preparation of L-Cys(*t*Bu)-OH based organogel

To prepare different percentages of organogels from 3 to 6 wt/v% for the L-Cys(*t*Bu)-OH based organogels, different weights of L-Cys(*t*Bu)-OH were dissolved in 0.25 mL sunflower oil in an Eppendorf tube and were put in an ultrasonic bath 35 °C for 20 minutes and gel formation occurred spontaneously. If the 10 M NaOH was added as the base, the sonication time was decreased to 1 minute. To test the gel formation, an inversion test was used [29].

3.7.3 Preparation of L-Cys(*t*-dodecyl-sulfanyl)-OH based organogel

To prepare different percentages of organogels from 0 to 5 wt/v% for the L-Cys(*t*-dodecyl-sulfanyl)-OH based organogels, different weights of L-Cys(*t*-dodecyl-sulfanyl)-OH were dissolved in 0.15 mL sunflower oil in an Eppendorf tube followed by adding different amounts of 10 M NaOH as the base. The tubes were put in an ultrasonic bath 45 °C for 10 minutes and gel formation occurred spontaneously. To test the gel formation, an inversion test was used [29].

3.8 Characterization of organogels

3.8.1 Transmission electron microscopy (TEM) imagining

5 wt/v% L-Cys(S*t*Bu)-OH based gel in THF and 5 wt/v% L-Cys(*t*-dodecyl-sulfanyl)-OH based gel in sunflower oil were prepared and diluted 50-fold with THF. then they were applied on a Cu grid and the excess solution was evaporated after 2 minutes and were stained with 2% uranyl acetate solution for another 2 minutes and washed with MiliQ water 2 times. FEI Tecnai G2 Spirit BioTwin CTEM microscope was used to image the fibrillar formations after self-assembly of the organogels.

3.8.2 X-ray diffraction analysis (XRD) measurements

The physicochemical nature of the formulations was studied by X-ray diffraction (XRD) measurement to show the morphology of the formulations in their native state. XRD measurements were conducted using X'Pert³ MRD with Cu Kα X-ray radiation (λ = 1.5406 Å). 5 wt/v% L-Cys(S*t*Bu)-OH in THF was prepared and dried using a freeze-drier to obtain xerogel. 5 wt/v% L-Cys(*t*-dodecyl-sulfanyl)-OH in sunflower oil was prepared and diluted in THF and dried under reduced pressure to obtain xerogel. The formulations were spread evenly over a glass plate and then subjected to X-ray analysis. The distance of hydrogen and Van der Waals bonds were calculated using [interplanar spacing (d) = order of reflection (n) × wavelength (λ) / 2 × sinθ] formula.

3.8.3 Rheological measurements

Gelation kinetics of the L-Cys(S*t*Bu)-OH and L-Cys(*t*-dodecyl-sulfanyl)-OH based organogels was determined by a time-sweep test within the linear viscoelastic range using Physica MCR 301, Anton Paar. 5 wt/v% L-Cys(S*t*Bu)-OH and L-Cys(*t*-

dodecyl-sulfanyl)-OH based organogels were prepared in sunflower oil. Storage modulus (G′) and loss modulus (G″) were monitored under a strain sweep of 0.01−500% at a frequency of 10 rad/s at 25 °C.

3.8.4 Drug release kinetics of the organogels

3.8.4.1 Drug release kinetics of the DOX loaded 6 wt/v% L-Cys(S*t*Bu)-OH based organogels

Six tubes of DOX loaded 6 wt/v% L-Cys(S*t*Bu)-OH based organogels and six tubes of DOX loaded 6 wt/v% L-Cys(*t*Bu)-OH based organogels in sunflower oil were prepared by adding 60 µL of the 0.006 g doxorubicin in 1.2 mL propylene glycol solution into 0.015 g of organogelators (L-Cys(S*t*Bu)-OH and L-Cys(*t*Bu)-OH) and 0.25 mL sunflower oil in Eppendorf tubes. The organogels were formed using a 35 °C sonic bath for 20 minutes and were stirred overnight.

Organogels were divided into two groups; EXP1, containing 3 tubes of DOX loaded 6 wt/v% L-Cys(S*t*Bu)-OH based organogel and 3 tubes of DOX loaded 6 wt/v% L-Cys(*t*Bu)-OH based organogel. 1 mL of the 0.025 g GSH in 30 mL PBS with pH 7.2 was added on top of the gels. And EXP2, containing 3 tubes of DOX loaded 6 wt/v% L-Cys(S*t*Bu)-OH based organogel and 3 tubes of DOX loaded 6 wt/v% L-Cys(*t*Bu)-OH based organogel. 1 mL of the 0.075 g GSH in 30 mL PBS with pH 7.2 was added on top of the gels. 100 µL of the PBS-GSH solutions from the top of the gels was removed and replaced with 100 µL fresh PBS-GSH solution every 15 minutes for the first 90 minutes and every 30 minutes for the next 6.5 hours, followed by taking samples at 24, 48, 72, 144, and 312 hours. 100 µL PBS was used as the negative control. 60 µL of the 0.006 g doxorubicin in 1.2 mL propylene glycol was poured into 1 mL PBS, and 100 µL of this solution was used as the positive control. The absorbance of doxorubicin released into the PBS solution on the top of the gels was measured at 480 nm using a BioTek epoch 2 microplate reader. Statistical analyses were performed and the error bars indicate the standard error of the mean.

3.8.4.2 Drug release kinetics of the DOX loaded 6 wt/v% L-Cys(*t*-dodecyl-sulfanyl)-OH based organogels

Six tubes of DOX loaded 6 wt/v% L-Cys(*t*-dodecyl-sulfanyl)-OH based organogels and six tubes of DOX loaded 6 wt/v% L-Cys(*t*Bu)-OH based organogels in sunflower oil were prepared by adding 13 µL 10 M NaOH to 0.012 g of organogelators (L-Cys(*t*-dodecyl-sulfanyl)-OH and L-Cys(*t*Bu)-OH) and 0.2 mL sunflower oil in Eppendorf tubes. The organogels were formed using a 45 °C sonic bath for 10 minutes for L-Cys(*t*-dodecyl-sulfanyl)-OH based organogels and a 35 °C sonic bath for 1 minute for L-Cys(*t*Bu)-OH based organogels. The organogels stirred overnight at room temperature followed by injecting 10 µL of the 0.006 g doxorubicin in 0.2 mL propylene glycol solution in the middle of the gels and stirring overnight.

Organogels were divided into two groups; EXP1, containing 3 tubes of DOX loaded 6 wt/v% L-Cys(*t*-dodecyl-sulfanyl)-OH based organogel and 3 tubes of DOX loaded 6 wt/v% L-Cys(*t*Bu)-OH based organogel. 1 mL of the 0.025 g GSH in 30 mL PBS with pH 7.2 was added on top of the gels. And EXP2, containing 3 tubes of DOX loaded 6 wt/v% L-Cys(*t*-dodecyl-sulfanyl)-OH based organogel and 3 tubes of DOX loaded 6 wt/v% L-Cys(*t*Bu)-OH based organogel. 1 mL of the 0.075 g GSH in 30 mL PBS with pH 7.2 was added on top of the gels. 100 µL of the PBS-GSH solutions from the top of the gels was removed and replaced with 100 µL fresh PBS-GSH solution every 15 minutes for the first 90 minutes and every 30 minutes for the next 6.5 hours, followed by taking samples at 24, 48, 72, 144, and 312 hours. 100 µL PBS was used as the negative control. 10 µL of the 0.006 g doxorubicin in 0.2 mL propylene glycol was poured into 1 mL PBS, and 100 µL of this solution was used as the positive control. The absorbance of doxorubicin released into the PBS solution on the top of the gels was measured at 480 nm for L-Cys(*t*Bu)-OH based organogels and at 480±20 nm for L-Cys(*t*-dodecyl-sulfanyl)-OH based organogels using a BioTek epoch 2 microplate reader. Statistical analyses were performed and the error bars indicate the standard error of the mean.

3.8.5 In vitro biocompatibility study of organogelators

Biocompatibility of the organogelators was carried out using the L929 cell line. 10×10^3 cells were seeded in each well of the 96 well plates containing DMEM and 10 % FBS and the cells were allowed to attach for 24 hours. 10 mg of L-Cys(S*t*Bu)-OH, L-Cys(*t*-dodecyl-sulfanyl)-OH, and L-Cys-OH were sterilized under the UV light for 20 minutes and were dissolved directly in 1 mL of the DMEM full medium as the main stock and were filtered using 0.22-micron filters. The cells were treated with L-Cys(S*t*Bu)-OH, L-Cys(*t*-dodecyl-sulfanyl)-OH, and L-Cys-OH with the final concentrations of 1 μM, 10 μM, 50 μM, 100 μM, 500 μM, 1 mM, and 5 mM in each well and the negative control cells included untreated cells (Figure 26). The plates were incubated in a CO_2 incubator (5% CO_2) and maintained at 37 °C for 24 and 48 hours. After 24 and 48 hours of treatment, cells were incubated in the culture medium containing 10% MTT (3-(4,5-dimethylthiazol-2-yl)- 2,5-diphenyltetrazolium bromide) for 4 hours, which resulted in the formation of formazan crystals. The crystals were solubilized in SDS overnight and then the absorbance of the dye was measured at 570 nm using the ThermoScientific plate reader. Statistical analyses were performed using two-way ANOVA. The level of statistical significance is represented by ns for $p > 0.05$, * for $p < 0.05$, ** for $p < 0.01$, *** for $p < 0.001$, and **** for $p < 0.0001$. Error bars indicate the standard error of the mean.

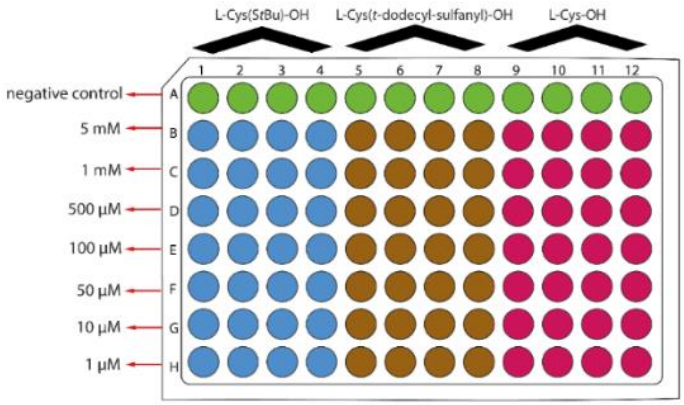

Figure 26: 96 well plate design for in vitro biocompatibility study of the organogelators.

REFERENCES

1. Yi, X.; Zeng, W.; Wang, C.; Chen, Y.; Zheng, L.; Zhu, X.; Ke, Y.; He, X.; Kuang, Y.; Huang, Q. A step-by-step multiple stimuli-responsive metal-phenolic network prodrug nanoparticles for chemotherapy. *Nano. Res*. **2022**, *15*, 1205.
2. Peter, S.; Alven, S.; Maseko, R. B.; Aderibigbe, B. A. Doxorubicin-Based Hybrid Compounds as Potential Anticancer Agents: A Review. *Molecules.* **2022**, *27*, 4478.
3. Nikolakakis, I.; Partheniadis, I. Self-Emulsifying Granules, and Pellets: Composition and Formation Mechanisms for Instant or Controlled Release. *Pharmaceutics.* **2017**, *9*, 50.
4. Bulbake, U.; Doppalapudi, S.; Kommineni, N.; Khan, W. Liposomal Formulations in Clinical Use: An Updated Review. *Pharmaceutics.* **2017**, *9*, 12.
5. Tenchov, R.; Bird, R.; Curtze, A. E.; Zhou, Q. Lipid Nanoparticles-From Liposomes to mRNA Vaccine Delivery, a Landscape of Research Diversity and Advancement. *ACS. Nano*. **2021**, *15*, 16982.
6. Uddin, S.; Islam, M. R.; Md Moshikur, R.; Wakabayashi, R.; Kamiya, N.; Moniruzzaman, M.; Goto, M. Transdermal Delivery of Antigenic Protein Using Ionic Liquid-Based Nanocarriers for Tumor Immunotherapy. *ACS. Appl. Bio. Mater*. **2022**, *5*, 2586.
7. Haddadzadegan, S.; Dorkoosh, F.; Bernkop-Schnürch, A. Oral delivery of therapeutic peptides and proteins: Technology landscape of lipid-based nanocarriers. *Adv. Drug Deliv. Rev*. **2022**, *182*, 114097.
8. Eun, Y. J.; Utada, A. S.; Copeland, M. F.; Takeuchi, S.; Weibel, D. B. Encapsulating Bacteria in Agarose Microparticles Using Microfluidics for High-Throughput Cell Analysis and Isolation. *ACS. Chem. Biol.* **2011**, *6*, 260.
9. He, P.; Liu, J.; Liu, K.; Ding, L.; Yan, J.; Gao, D.; Fang, Y. Preparation of novel organometallic derivatives of cholesterol and their gel-formation properties. *Colloids. Surf.* **2010**, *362*, 127.

10. Nurchi, C.; Buonvino, S.; Arciero, I.; Melino, S. Sustainable Vegetable Oil-Based Biomaterials: Synthesis and Biomedical Applications. *Int. J. Mol. Sci.* **2023**, *24*, 2153.
11. Esposito, C. L.; Tardif, V.; Sarrazin, M.; Kirilov, P.; Roullin, V. G. Preparation and characterization of 12-HSA-based organogels as injectable implants for the controlled delivery of hydrophilic and lipophilic therapeutic agents. *Mater. Sci. Eng. C.* **2020**, *114*, 110999.
12. Siafaka, P. I.; Gündoğdu, E. A.; Cağlar, E. S.; Özgenç, E.; Gonzalez-Alvarez, M.; Gonzalez-Alvarez, I.; Okur, N. Ü. Polymer-based Gels: Recent and Future Applications in Drug Delivery Field. *Curr. Drug. Deliv.* **2023**, *20*, 1288.
13. Sagiri, S. S.; Behera, B.; Rafanan, R. R.; Bhattacharya, C.; Pal, K.; Banerjee, I.; Rousseau, D. Organogels as Matrices for Controlled Drug Delivery: A Review on the Current State. *Soft. Mater.* **2014**, *12*, 47.
14. Marr, P. C.; Marr, A. C. Ionic liquid gel materials: applications in green and sustainable chemistry. *Green. Chem.* **2016**, *18*, 105.
15. Kowalczuk, J.; Bielejewski, M.; Lapiński, A.; Luboradzki, R.; Tritt-Goc, J. The solvent-gelator interaction is the origin of different diffusivity behavior of diols in gels formed with sugar-based low-molecular-mass gelator. *J. Phys. Chem. B.* **2014**, *118*, 4005.
16. Coubrough, H. M.; Jones, C. D.; Yufit, D. S.; Steed, J. W. Gelation by histidine-derived ureas. *Supramol. Chem.* **2018**, *30*, 384.
17. Buerkle, L. E.; Rowan, S. J. Supramolecular gels formed from multi-component low molecular weight species. *Chem. Soc. Rev.* **2012**, *41*, 6089.
18. Lan, Y.; Corradini, M. G.; Weiss, R. G.; Raghavan, S. R.; Rogers, M. A. To gel or not to gel: correlating molecular gelation with solvent parameters. *Chem. Soc. Rev.* **2015**, *44*, 6035.
19. Draper, E. R.; Adams, D. J. Low-Molecular-Weight Gels: The State of the Art. *Chem.* **2017**, *3*, 390.
20. Li, X.; Saleh, S. M. A.; Wang, P.; Wang,Q.; Yang, S.; Zhu,M.; Duan, Y.; Xiao, Z. Characterization of Organogel Prepared from Rice Bran Oil with Cinnamic Acid.

Food. Biophys. **2017**, *12*, 356.

21. Terech, P.; R.G. Weiss. Low molecular mass gelators of organic liquids and the properties of their gels. *Chem. Rev.* **1997**, *97*, 3133.
22. George, M.; R.G. Weiss. Molecular organogels. Soft matter comprised of low-molecular-mass organic gelators and organic liquids. *Acc. Chem. Res.* **2006**, *39*, 489.
23. Liu, K.; Yan, N.; Peng, J.; Liu, J.; Zhang, Q.; Fang, Y. Supramolecular gels based on organic diacid monoamides of cholesteryl glycinate. *J. Colloid. Interface. Sci.* **2008,** *327*, 233.
24. Tu, T.; Assenmacher, W.; Peterlik, H.; Weisbarth, R.; Nieger, M.; Dötz, K. H. An Air-Stable Organometallic Low-Molecular-Mass Gelator: Synthesis, Aggregation, and Catalytic Application of a Palladium Pincer Complex. *Angew. Chem., Int. Ed.* **2007**, *46*, 6368.
25. Li, Y. G.; Liu, K. Q.; Liu, J.; Peng, J. X.; Feng, X. L.; Fang, Y. Amino Acid Derivatives of Cholesterol as "Latent" Organogelators with Hydrogen Chloride as a Protonation Reagent. *Langmuir*. **2006**, *22*, 7016.
26. Löfman, M.; Koivukorpi, J.; Noponen, V.; Salo, H.; Sievänen, E. Bile acid alkylamide derivatives as low molecular weight organogelators: Systematic gelation studies and qualitative structural analysis of the systems. *J. Colloid Interface Sci.* **2011**, *360*, 633.
27. Suzuki, M.; Nigawara, T.; Yumoto, M.; Kimura, M.; Shirai, H.; Hanabusa, K. New gemini organogelators linked by oxalyl amide: organogel formation and their thermal stabilities. *Tetrahedron. Lett.* **2003**, *44*, 6841.
28. Brosse, N.; D. Barth; B. Jamart-Grégoire. A family of strong low-molecular-weight organogelators based on amino acid derivatives. *Tetrahedron. Lett.* **2004**, *45*, 9521.
29. Aykent, G.; Zeytun, C.; Marion, A.; Özçubukçu, S. Simple Tyrosine Derivatives Act as Low Molecular Weight Organogelators. *Sci. Rep*. **2019**, *9*, 4893.
30. Bastiat, G.; Leroux, J. C. Pharmaceutical organogels prepared from aromatic amino acid derivatives. *J. Mater. Chem.* **2009**, *19*, 3867.
31. Willimann, H. L.; P. L. Luisi. Lecithin organogels as a matrix for the transdermal transport of drugs. *Biochem. Biophys. Res. Commun.* **1991**, *177*, 897.

32. Bot, A.; A. R. den; E. Roijers. Fibrils of γ-Oryzanol + β-Sitosterol in edible oil organogels. *J. Am. Oil. Chem. Soc.* **2008**, *85*, 1127.
33. Yoza, K.; Ono, Y.; Yoshihara, K.; Akao, T.; Shinmori, H.; Takeuchi, M.; Shinkai, S.; Reinhoudt, D. Sugar-integrated gelators of organic fluids on their versatility as building-blocks and diversity in superstructures. *Chem. Commun.* **1998**, *8*, 907.
34. Murdan, S. Organogels in drug delivery. *Expert. Opin. Drug. Deliv.* **2005**, *2*, 489.
35. van Esch, J. H.; Feringa, B. L. New Functional Materials Based on Self-Assembling Organogels: From Serendipity towards Design. *Angew. Chem. Int. Ed.* **2000**, *39*, 2263.
36. Skilling, K. J.; Citossi, F.; Bradshaw, T. D.; Ashford, M. B.; Kellam, B.; Marlow, M. Insights into low molecular mass organic gelators: a focus on drug delivery and tissue engineering applications. *Soft. Mater.* **2014**, *10*, 237.
37. Vibhute, A. M.; Muvvala, V.; Sureshan, K. M. A Sugar-Based Gelator for Marine Oil-Spill Recovery. *Angew. Chem*. **2016**, *55*, 7782.
38. Hirst A. R.; Escuder B.; Miravet J. F.; Smith D. K. High-tech applications of self-assembling supramolecular nanostructured gel-phase materials: from regenerative medicine to electronic devices. *Angew. Chem. Int. Ed. Engl*. **2008**,*47*, 8002.
39. Jones, C. D.; Steed, J. W. Gels with sense: supramolecular materials that respond to heat, light, and sound. *Chem. Soc. Rev*. **2016**, *45*, 6546.
40. Li, Z.; Cao, J.; Li, H.; Liu, H.; Han, F.; Liu, Z.; Tong, C.; Li, S. Self-assembled drug delivery system based on low-molecular-weight bis-amide organogelator: synthesis, properties and in vivo evaluation. *Drug. Deliv*. **2016**, *23*, 3168.
41. Taylor, M.; Tomlins, P.; Sahota, T. Thermoresponsive Gels. *Gels.* **2017**,*3*, 4.
42. Ngai, T.; Bon, S. Eds. The Phenomenon of Pickering Stabilization: A Basic Introduction. In Particle-Stabilized Emulsions and Colloids: Formation and Applications. *RSC. Soft. Matter. Series*. Cambridge, UK, **2014**.
43. Basak, S.; Nanda, J.; Banerjee, A. A new aromatic amino acid based organogel for oil spill recovery. *J. Mater. Chem.* **2012**, *22*, 11658.
44. Yeingst T. J.; Arrizabalaga J. H.; Hayes D. J. Ultrasound-Induced Drug Release from Stimuli-Responsive Hydrogels. *Gels*. **2022**, *8*, 554.

45. P.K. Bolla; V.A. Rodriguez; R.S. Kalhapure; C.S. Kolli; S. Andrews; J. Renukuntla . A review on pH and temperature responsive gels and other less explored drug delivery systems. *J. Drug. Deliv. Sci. Technol.* **2018**, *46*, 416.
46. Kiyonaka, S.; Sugiyasu, K.; Shinkai, S.; Hamachi, I. First thermally responsive supramolecular polymer based on glycosylated amino acid. *J. Am. Chem. Soc.* **2002**, *124*, 10954.
47. Brinksma, J.; Feringa, B. L.; Kellogg, R. M.; Vreeker, R.; Van Esch, J. Rheology and thermotropic properties of bis-urea-based organogels in various primary alcohols. *Langmuir.* **2000**, *16*, 9249.
48. Cravotto, G.; Cintas, P. Molecular self-assembly and patterning induced by sound waves. The case of gelation. *Chem. Soc. Rev.* **2009**, *38*, 2684.
49. Murata, K.; Aoki, M.; Suzuki, T.; Harada, T.; Kawabata, H.; Komori, T.; Ohseto, F.; Ueda, K.; Shinkai, S. Thermal and Light Control of the Sol-Gel Phase Transition in Cholesterol-Based Organic Gels. Novel Helical Aggregation Modes As Detected by Circular Dichroism and Electron Microscopic Observation. *J. Am. Chem. Soc.* **1994**, *116*, 6664.
50. Yan-Li Zhao; J. Fraser Stoddart. Azobenzene-Based Light-Responsive Hydrogel System. *Langmuir*. **2009**, *25*, 8442.
51. Kitamura, T.; Nakaso, S.; Mizoshita, N.; Tochigi, Y.; Shimomura, T.; Moriyama, M.; Ito, K.; Kato, T. Electroactive supramolecular self-assembled fibers comprised of doped tetrathiafulvalene-based gelators. *J. Am. Chem. Soc.* **2005**, *127*, 14769.
52. Fukino, T.; Yamagishi, H.; Aida, T. Redox-Responsive Molecular Systems and Materials. *Adv. Mater.* **2017**, *29*, 1603888.
53. Guo, X.; Cheng, Y.; Zhao, X.; Luo, Y.; Chen, J.; Yuan, W. E. Advances in redox-responsive drug delivery systems of tumor microenvironment. *J. Nanobiotechnology.* **2018**, *16*, 1.
54. Luo, C.; Sun, J.; Liu, D.; Sun, B.; Miao, L.; Musetti, S.; Li, J.; Han, X.; Du, Y.; Li, L.; Huang, L.; He, Z. Self-Assembled Redox Dual-Responsive Prodrug-Nanosystem Formed by Single Thioether-Bridged Paclitaxel-Fatty Acid Conjugate for Cancer Chemotherapy. *Nano. Lett.* **2016**, *16*, 5401.

55. Estrela, J. M.; Ortega, A.; Obrador, E. Glutathione in cancer biology and therapy. *Crit. Rev. Clin. Lab. Sci.* **2006**, *43*, 143.
56. Xue, Q.; Ye, C.; Zhang, M.; Hu, X.; Cai, T. Glutathione responsive cubic gel particles cyclodextrin metal-organic frameworks for intracellular drug delivery. *J. Colloid. Interface. Sci.* **2019**, *551*, 39.
57. Traverso, N.; Ricciarelli, R.; Nitti, M.; Marengo, B.; Furfaro, A. L.; Pronzato, M. A.; Marinari, U. M.; Domenicotti, C. Role of glutathione in cancer progression and chemoresistance. *Oxid. Med. Cell. Longev.* **2013**, 972913.
58. Elda Valenti, G.; Tasso, B.; Traverso, N.; Domenicotti, C.; Marengo, B. Glutathione in cancer progression and chemoresistance: an update. *Redox. Experimental. Medicine*. **2023**, *1*, 220023.
59. Yue, D.; Cheng, G.; He, Y.; Nie, Y.; Jiang, Q.; Cai, X.; Gu, Z. Influence of reduction-sensitive diselenide bonds and disulfide bondson oligo ethylenimine conjugates for gene delivery. *J. Mater. Chem. B*. **2014**, *2*, 7210.
60. Alarifi, S.; Ali, D. Mechanisms of Multi-walled Carbon Nanotubes-Induced Oxidative Stress and Genotoxicity in Mouse Fibroblast Cells. *Int. J. Toxicol.* **2015**, *34*, 258.
61. Sevim, Ç.; Taghizadehghalehjoughi, A.; Kara, M. In Vitro Investigation of the Effects of Imidacloprid on AChE, LDH, and GSH Levels in the L-929 Fibroblast Cell Line. *Turk. J. Pharm. Sci*. **2020**, *17*, 506.
62. Carvalho, F. S.; Burgeiro, A.; Garcia, R.; Moreno, A. J.; Carvalho, R. A.; Oliveira, P. J. Doxorubicin-Induced Cardiotoxicity: From Bioenergetic Failure and Cell Death to Cardiomyopathy. *Med. Res. Rev.* **2014**, *34*, 106.
63. Thorn, C. F.; Oshiro, C.; Marsh, S.; Hernandez-Boussard, T.; McLeod, H.; Klein, T. E.; Altman, R.B. Doxorubicin pathways: pharmacodynamics and adverse effects. *Pharmacogenet. Genomics*. **2011**, *21*, 440.
64. Postma, T. M.; Giraud, M.; Albericio, F. Trimethoxyphenylthio as a Highly Labile Replacement for *tert*-Butylthio Cysteine Protection in Fmoc Solid Phase Synthesis. *Org. Lett.* **2012**,*14*, 5468.

65. Chakraborty, A.; Sharma, A.; Albericio, F.; de la Torre, B. G. Disulfide-Based Protecting Groups for the Cysteine Side Chain Amit Chakraborty. *Org. Lett.* **2020**, *22*, 9644.

APPENDICES A

NMR DATA

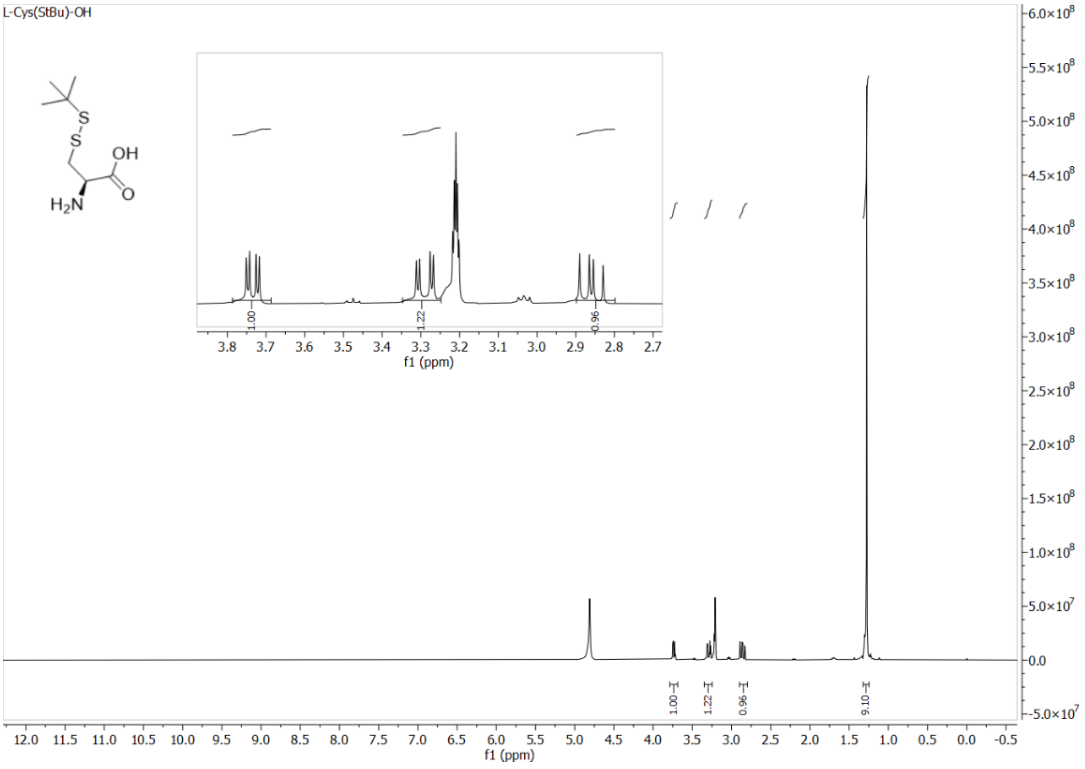

Figure A.1: ^{1}H NMR spectrum of L-Cys(S*t*Bu)-OH in MeOD.

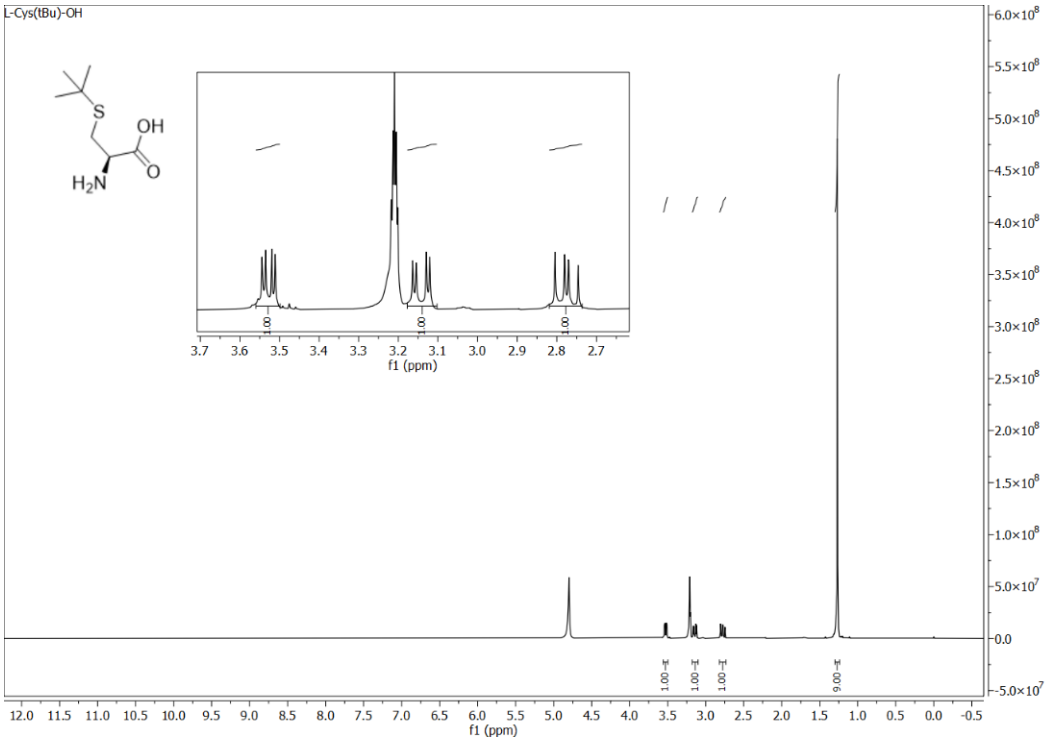

Figure A.2: ^{1}H NMR spectrum of L-Cys(*t*Bu)-OH in MeOD.

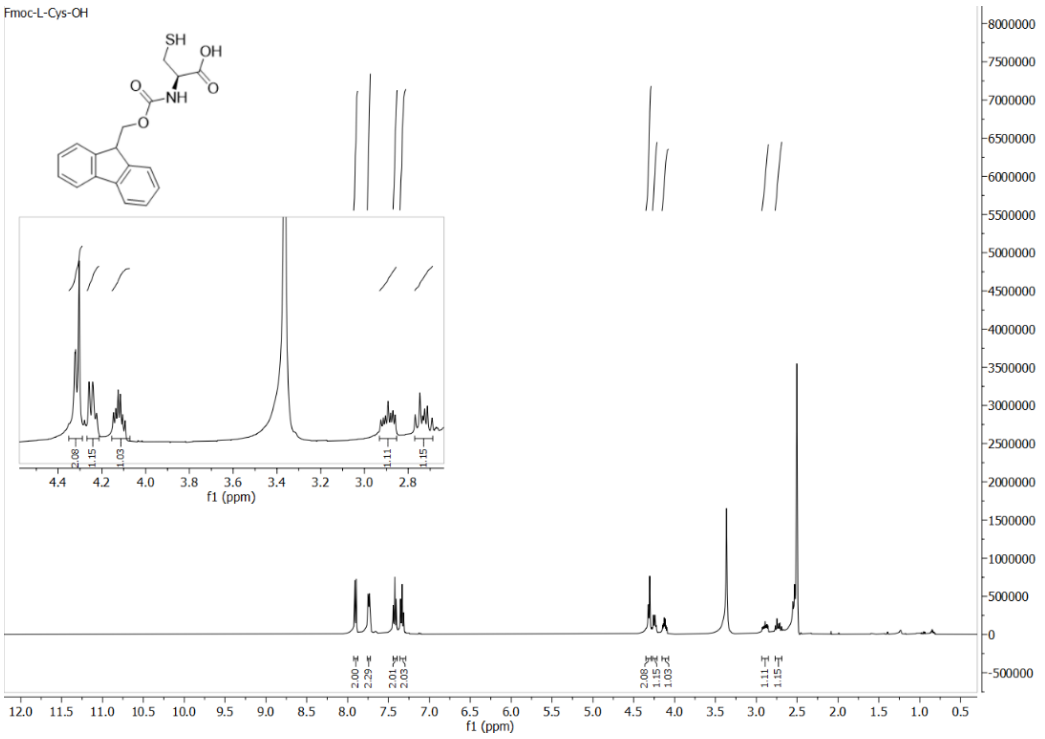

Figure A.3: ^{1}H NMR spectrum of Fmoc-L-Cys-OH in d_6-DMSO.

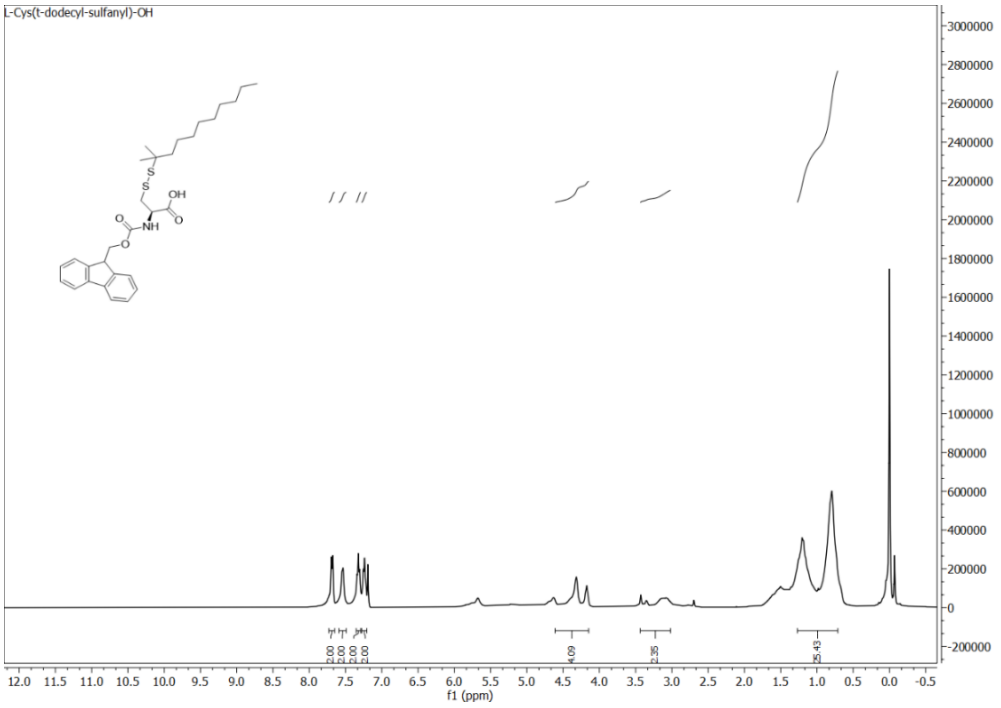

Figure A.4: ^{1}H NMR spectrum of Fmoc-L-Cys(*t*-dodecyl-sulfanyl)-OH in $CDCl_3$.

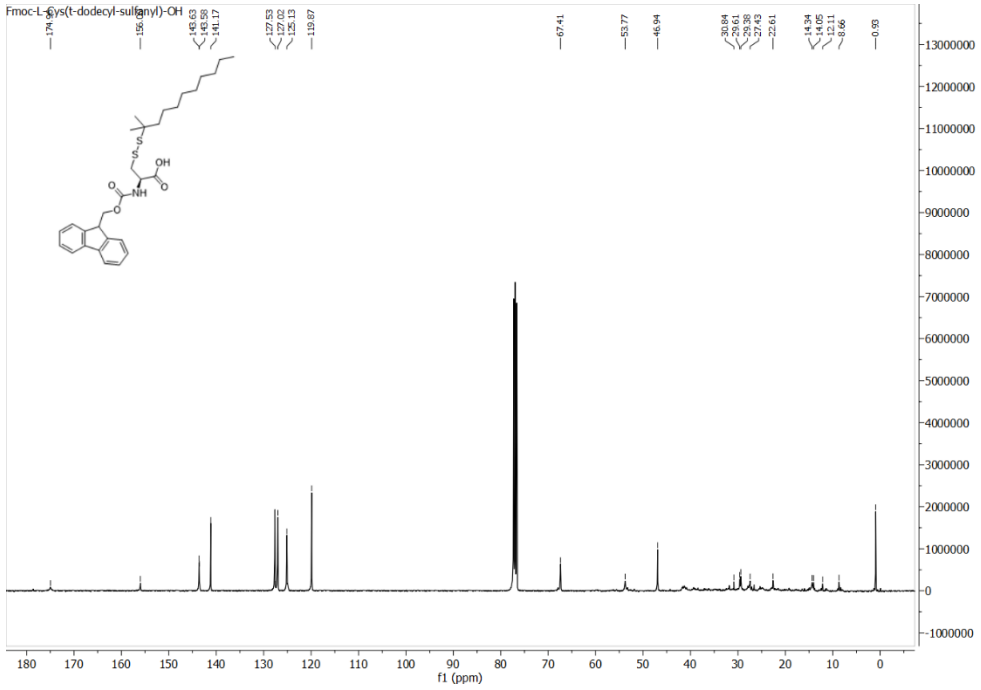

Figure A.5: ^{13}C NMR spectrum of Fmoc-L-Cys(*t*-dodecyl-sulfanyl)-OH in $CDCl_3$.

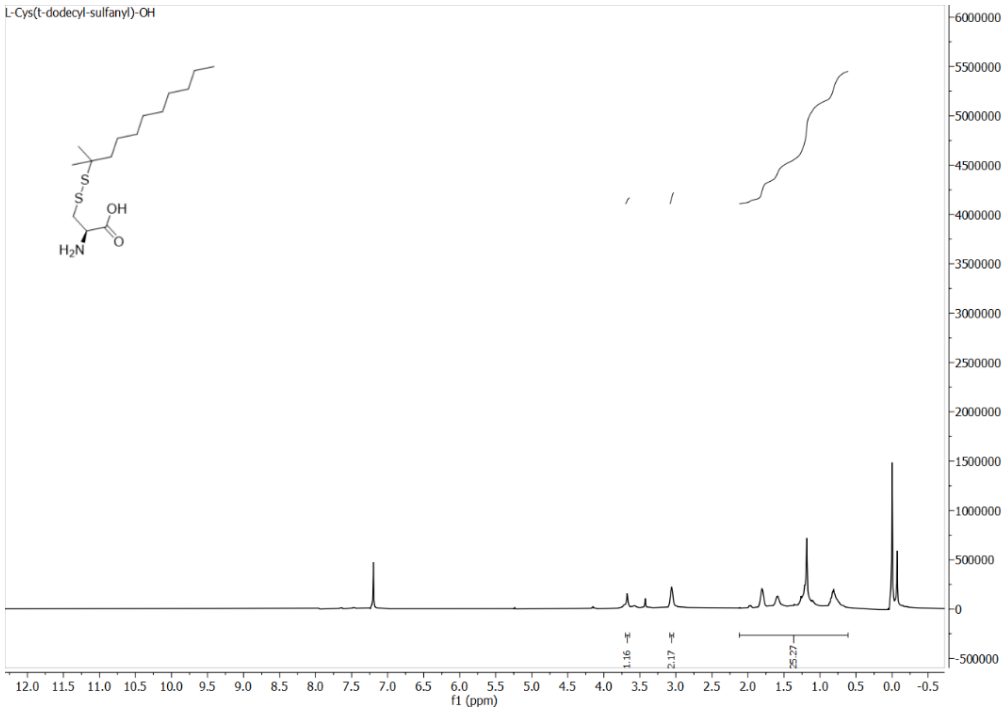

Figure A.6: ^{1}H NMR spectrum of L-Cys(*t*-dodecyl-sulfanyl)-OH in $CDCl_3$.

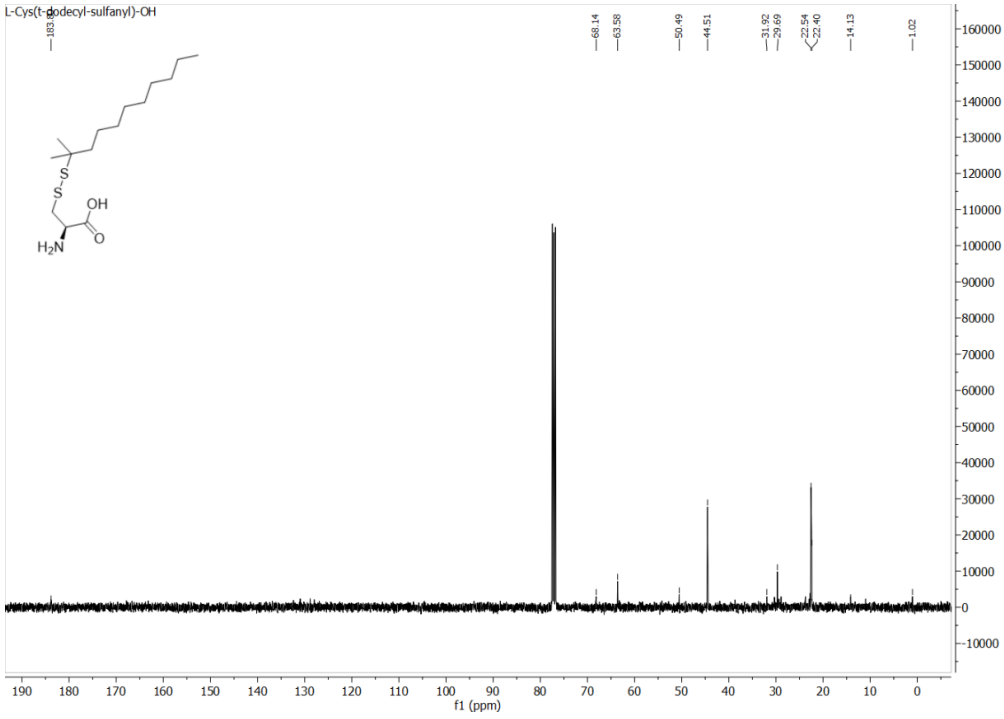

Figure A.7: ^{13}C NMR spectrum of L-Cys(*t*-dodecyl-sulfanyl)-OH in $CDCl_3$.

APPENDICES B

HRMS DATA

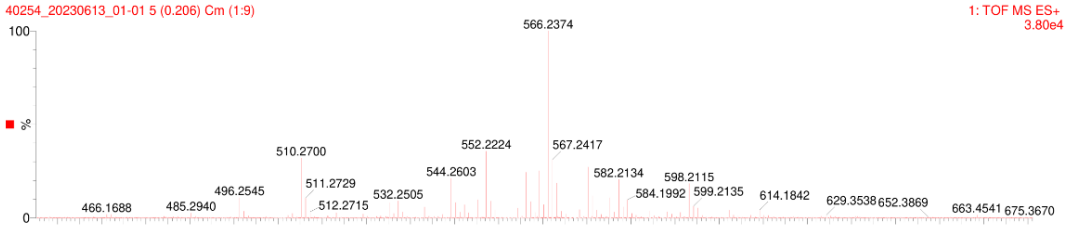

Figure B.1: HRMS chromatogram of Fmoc-L-Cys(*t*-dodecyl-sulfanyl)-OH.

Figure B.2: HRMS chromatogram of L-Cys(*t*-dodecyl-sulfanyl)-OH.